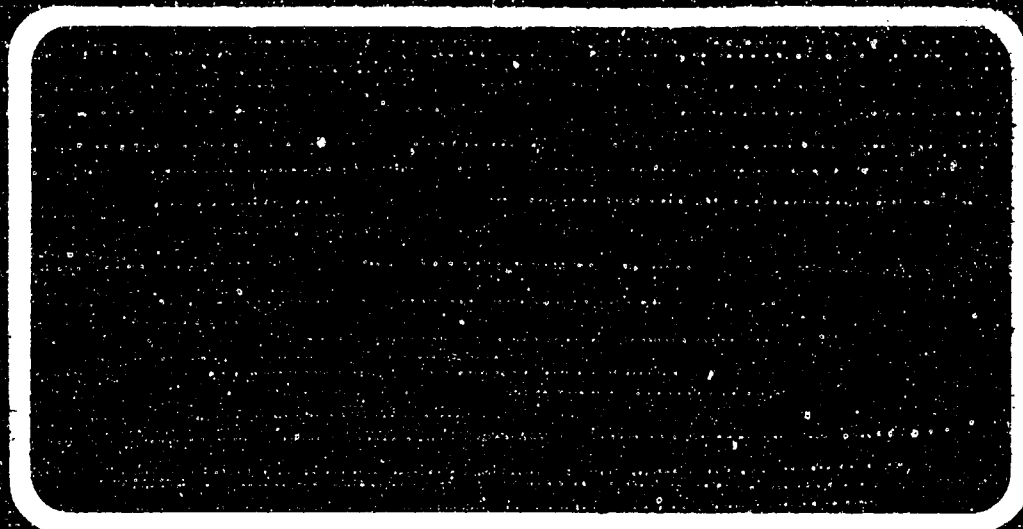


AD615789



ALCOA

ALCOA RESEARCH LABORATORIES

ALUMINUM COMPANY OF AMERICA

ALUMINUM COMPANY OF AMERICA
Alcoa Research Laboratories
Chemical Metallurgy Division
New Kensington, Pennsylvania

INVESTIGATION OF THE MECHANISM OF
STRESS CORROSION OF ALUMINUM ALLOYS

Bureau of Naval Weapons Contract Now64-0170c

This report may be released to OTS.

Final Report

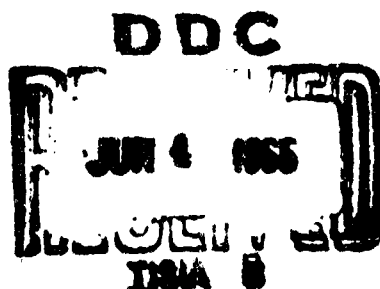
(Period of December 6, 1963, to February 6, 1965)

103-P

COPY	2	OF	3
HARD COPY	\$.	4.00	
MICROFILME	\$.	0.75	

Reported by: G. C. English
G. C. English

Approved by: E. H. Hollingsworth
E. H. Hollingsworth



ARCHIVE COPY.

ERRATA - Investigation of the Mechanism of Stress
Corrosion of Aluminum Alloys. Bureau of Naval Weapons
Contract NOW 64-0170-c. Final Report,
December 6, 1963, to February 6, 1965.

1. Page 3, paragraph 3, line 3 - insert "as" between "added" and "50."
2. Page 23, paragraph 1, line 4 - change "Kologyrkin" to "Kolotyrrkin."
3. Page 23, paragraph 2, line 7 - change "importnat" to "important."
4. Table III, next to last entry - change "-1290" to "(-1290*)."
5. Figure 9, facing sheet caption - add "The stressed specimen was stressed to 75% of the yield strength."
6. Figure 20, facing sheet caption, last sentence - change to "Any gray particles like those shown at "A" in Figure 19 appear to have dissolved out."
7. Figure 23, facing sheet caption, line 3 - change Figure 18 to Figure 22.
8. Figure 23, facing sheet caption, line 6 - change Figure 15 to Figure 19.
9. Figure 24, facing sheet caption, line 3 - change Figures 18 and 19 to Figures 22 and 23.
10. Figure 24, facing sheet caption, line 5 - change Figure 15 to Figure 19.
11. Figure 24, facing sheet caption, lines 7 and 8 - change "The particles at "A" have been attacked. Originally these particles were similar to those shown at "A" in Figure 19."
12. Figure 24, facing sheet caption, line 11 - change Figure 17 to Figure 21.
13. Figure 28 - The data point at pH 12 shown as an open circle should be a solid circle.

AD 615789

ERRATA - Investigation of the Mechanism of Stress
Corrosion of Aluminum Alloys. Bureau of Naval Weapons
Contract NOW 64-0170-c. Final Report,
December 6, 1963, to February 6, 1965.

1. Page 3, paragraph 3, line 3 - insert "as" between "added" and "50."
2. Page 23, paragraph 1, line 4 - change "Kologyrkin" to "Kolotyrkin."
3. Page 23, paragraph 2, line 7 - change "importnat" to "important."
4. Table III, next to last entry - change "-1290" to "(-1290*)."
5. Figure 9, facing sheet caption - add "The stressed specimen was stressed to 75% of the yield strength."
6. Figure 20, facing sheet caption, last sentence - change to "Any gray particles like those shown at "A" in Figure 19 appear to have dissolved out."
7. Figure 23, facing sheet caption, line 3 - change Figure 18 to Figure 22.
8. Figure 23, facing sheet caption, line 6 - change Figure 15 to Figure 19.
9. Figure 24, facing sheet caption, line 3 - change Figures 18 and 19 to Figures 22 and 23.
10. Figure 24, facing sheet caption, line 5 - change Figure 15 to Figure 19.
11. Figure 24, facing sheet caption, lines 7 and 8 - change "The particles at "A" have been attacked. Originally these particles were similar to those shown at "A" in Figure 19."
12. Figure 24, facing sheet caption, line 11 - change Figure 17 to Figure 21.
13. Figure 28 - The data point at pH 12 shown as an open circle should be a solid circle.

Table of Contents

	<u>Page</u>
Synopsis	
Introduction	1
Materials	2
Experimental	3
Results	10
Discussion	18
Tables I - VI	
Figures 1 - 32	
Appendix I	
Appendix II	

ALUMINUM COMPANY OF AMERICA
Alcoa Research Laboratories
Chemical Metallurgy Division
New Kensington, Pennsylvania

SYNOPSIS:

The cathodic protection of 7075 alloy in a corrosive, acid chloride solution was investigated. Subsize tensile specimens for protection were taken in the short-transverse direction from 2-inch thick plate in two tempers, one (-T6) susceptible to stress corrosion and one (-T73) not susceptible to this type of corrosion. In the solution used a susceptible specimen stressed to 75% of its yield strength failed by stress corrosion in an hour while a stressed non-susceptible specimen failed by general corrosion within two days.

At a potential 0.57 volts negative to the free corrosion potential, a stressed susceptible specimen could be protected for an indefinitely long period; one susceptible specimen stressed to 75% of its yield strength and held at this potential for 400 hours showed no evidence of stress corrosion. This potential of cathodic protection appeared to be independent of the stress applied to a specimen. Considerable evidence indicates that the potential reflected metallurgical structure rather than extraneous conditions such as the alkalinity produced by cathodic reactions. Corrosion in one of the alloys ($MgZn_2$) prepared to reproduce precipitating phases in 7075 alloy was not prevented by cathodic protection until the potential approached that required to prevent stress corrosion.

For all specimens, general corrosion decreased as cathodic protection was increased, rapidly at first, and then much more gradually. Pitting on a microscopic scale (100X) ceased by the time

SYNOPSIS (continued):

a potential 0.20 to 0.25 volts negative to the free corrosion potential was reached. Maximum protection against general corrosion was reached at the same potential required for protection against stress corrosion; here the rate was so low that it could not be established with assurance by the change in electrical resistance.

An accelerating effect of stress on a susceptible specimen became evident at an early stage even though, for most stresses and potentials of cathodic protection, the rate of corrosion was low. At a later stage, an hour or so before a specimen failed, all stresses accelerated corrosion according to the same exponential function; and this second stage developed independently of the original stress although the exposure period before it developed did depend upon this stress. These results suggest strain induced depolarization of the anodic reaction. Electron microscopic examination of pre-polished surfaces of cathodically protected specimens shows promise for relating the depolarization to microstructural features. One possibility is that the depolarization in the first stage is related to the minute pitting revealed in unstressed, susceptible specimens by electron microscopic examination that was not eliminated until the potential required to prevent corrosion was reached.

INTRODUCTION:

This report summarizes an investigation carried out at the Alcoa Research Laboratories under Bureau of Naval Weapons Contract Now 64-0170c. The investigation was fundamental in nature and directed toward providing a better understanding of the stress corrosion of aluminum. Its eventual goal was to establish more firmly the premise that the stress corrosion of an aluminum alloy depends, not upon metallurgical structure alone, nor upon the electrochemical characteristics of this structure alone, but rather upon these two factors acting together in a specific environment.

Experimentally, the investigation was concerned mainly with the cathodic protection of 7075 alloy in two tempers, one (-T6) susceptible to stress corrosion and one (-T73) not susceptible to this type of corrosion. Attention was directed specifically toward establishing the potential of cathodic protection just required to prevent corrosion or stress corrosion. Establishing this potential provided a means for determining the potential of the most anodic phase involved in corrosion or stress corrosion (assuming naturally that these processes in aluminum alloys are electrochemical, as is accepted generally). In theory, at least, corrosion or stress corrosion should stop whenever cathodic polarization equals or exceeds the potential of the most anodic phase involved in the processes. In the work on cathodic protection, attention was given to establishing that the protection reflected metallurgical structure rather than extraneous environmental effects such as alkalinity resulting from the protection. Attention was also given to the effect of stress upon cathodic

protection and to following the course of corrosion and stress corrosion, particularly with partial or complete cathodic protection.

Finally, some attention was directed to reproducing the solid solution and precipitating phases in 7075 and to a limited extent, to the cathodic protection of these phases.

MATERIALS:

Plate. Tensile specimens for cathodic protection studies were taken in the short-transverse direction from a production lot of 2-inch thick 7075-T651 alloy plate. Blanks from this plate ($1/4"$ x $1/4"$ x $2"$) were reheat-treated, quenched in cold water and artificially aged to the -T6 and -T73 tempers and then machined into $1/8$ -inch diameter tensile specimens. The chemical analysis of the plate and its tensile properties and electrical conductivities in the -T6 and -T73 tempers are summarized in Table I.

Phases. The ten alloys in Table II were prepared to duplicate phases in 7075 alloy. Four of them were intermetallic compounds in the composition range of the so-called M-phase, the equilibrium precipitating phase in 7075 alloy consisting of $MgZn_2$ and $CuMgAl$. All ten alloys were made from high purity metals and hardeners; beryllium was added to minimize the loss of magnesium.

A one-pound charge of each of the six solid solution alloys was melted at $1350^\circ F$ in a graphite crucible and, after fluxing with chlorine and skimming, cast into a $3/4"$ x $4"$ x $3\ 1/2"$ ingot. Each ingot was preheated 16 hours at $920^\circ F$, hot rolled at $775^\circ F$ to a thickness of $0.5"$, scalped, hot-rolled again at

775°F to a thickness of 0.25", annealed 2 hours at 775°F and finally cold-rolled into 0.064" thick sheet. The sheet was solution heat-treated 3 hours at 925°F and cold water quenched.

Each of the four M-alloys was prepared from a 300 gram charge melted at 1200°-1600°F in a graphite crucible. In an attempt to remove gas, each charge was first cast into another graphite crucible preheated beforehand to 900°F and re-melted. It was then cast into a third graphite crucible 0.5" diameter x 2" long. The small casting prepared in this way was put into a graphite container, sealed under argon in a glass tube and annealed 20 days at 450°C.

EXPERIMENTAL:

Solution. The test solution contained 1.00 mole per liter of sodium chloride and 0.21 mole per liter of aluminum chloride (added 50 g/l $\text{AlCl}_3 \cdot 6 \text{H}_2\text{O}$). The pH was adjusted to 1.0 by the addition of concentrated hydrochloric acid. A pH of 1.0 was selected because it provided a measurable rate of general corrosion, and, equally important, because it produced stress corrosion cracking rapidly in specimens of 7075-T6 stressed in the short-transverse direction. Because aluminum chloride was introduced into the solution as a corrosion product in varying degrees in most of the tests, it appeared reasonable to start with a solution in which aluminum chloride initially was present at a level high enough so that the concentration would remain essentially constant throughout a test.

Apparatus. The apparatus and circuits used for the cathodic protection experiments are shown in Figures 1 and 2,

The tests were conducted in battery jars, each containing 9 liters of solution. A sheet of Flexiglas with suitable openings was used to cover each jar and support the specimen, the anodes and a thermometer. The anodes were located in individual compartments separated from the main portion of the solution by fritted glass discs of medium porosity. Aluminum of 99.99% purity was used for the anodes in preference to platinum because aluminum chloride was considered less objectionable than chlorine as an anode reaction product. The solution in the anode compartments was discarded each day and replaced with fresh solution. The main portion of the battery jar was, in effect, the cathode compartment of the cell.

One of the objects in using a large volume of solution was to minimize the pH increase produced by the cathodic reactions. Daily pH adjustment by adding a few milliliters of concentrated hydrochloric acid was sufficient to hold the pH constant to within ± 0.05 pH unit or better. An entirely fresh solution was made up from time to time especially after an appreciable amount of corrosion had occurred.

The potentiostats used in the present work were electronic instruments with chopper-stabilized operational amplifiers, similar in design to the instrument described by Booman (1). A recorder was used to provide a continuous record of the current and by means of a timer and relay, the recorder was also used to monitor the continuity of a specimen several times each hour. A 1 ohm or 0.1 ohm shunt connected across the two potential terminals of the specimen was used for this purpose. A negligible current flowed through the shunt until a specimen broke. When a specimen

broke, a measurable portion of the protection current flowed through the shunt and provided an indication on the recorder.

The specimens were stressed in standard fixtures for 1/8-inch tensile specimens. The electrical resistance measurements required that a specimen be insulated from the stressing frame and that current and potential leads be attached. Either an anodic hard coating or ceramic washers provided electrical insulation between the specimen and the frame. The necessary leads were attached by percussion welding.

A photograph of a specimen is shown in Figure 3. The two potential leads needed for resistance measurements were attached, one at each end of the specimen, in the area between the threads and the reduced section. A separate lead similarly located was used as a direct connection to the potentiostat. With this arrangement IR drops in the leads carrying the resistance test current did not interfere with the operation of the potentiostat and vice versa. The current leads for the resistance measurement were welded to the cap nuts used to mount the specimen in the stressing fixture. Corrosion tests and measurements to evaluate the loss in strain demonstrated that the modified specimen and frame used in the present tests were equivalent in performance to the standard specimen and frame.

Figure 3 also shows a specimen ready for immersion in the test solution. As this figure shows, wax stop-off was applied in such a way that the entire reduced section of the specimen was exposed to the solution. Hydrogen bubbles occasionally tended to cling to the metal-wax junction. There was a remote possibility

that such clinging bubbles might act as a temporary screen and thus allow a stress crack to initiate. Accordingly, the junction between the wax and the exposed area was established outside the uniform part of the reduced section to minimize the possibility of spurious attack occurring in the region of highest stress.

Luggin capillaries were mounted through holes drilled in the side members of the frame and each tip was positioned 3 millimeters from the surface of the specimen. The tip diameter was about 1 millimeter. Smaller capillaries positioned 1 millimeter from the specimen were used initially but were finally discontinued when it was found that they tended to catch stray hydrogen bubbles evolved from the surface of the specimen. The resulting open circuit condition prevented the potentiostat from functioning properly with the result that the experiment in progress was lost. The utmost in reliability is imperative where long-time runs are conducted. The use of two capillaries was simply a precaution rather than a necessity. Both capillaries were connected to the same reservoir in which a saturated calomel electrode was located.

All the potential measurements included in this report are in terms of the saturated calomel reference electrode. The European sign convention is used in which the potential of an active metal is given a negative sign. A Leeds and Northrup 8687 potentiometer was used to measure electrode potentials.

Correction for IR Drops. At the current densities encountered, it was necessary to apply a correction for the IR drop in the solution between the capillary tip and the specimen. By means of a movable capillary,

it was found that the potential distribution followed the ideal law for concentric cylinders for distances up to about 1 centimeter from the surface of the specimen. The resistance could be calculated from the following equation:

$$R = \frac{\rho}{2\pi} \ln (r_2/r_1) \quad (1)$$

where ρ is the resistivity of the solution (7.86 ohm-cm at 25°C), r_1 is the radius of the specimen in centimeters, r_2 is the corresponding radius out to the tip of the Luggin capillary and R is the resistance of an annular cylinder of solution surrounding the specimen and having the following dimensions: height of 1 centimeter, inner diameter of $2r_1$ and outer diameter of $2r_2$. The correction to the measured potential is then the product $I \times R$, where R is given by equation (1) and I is the current flowing to the corresponding area. Expressed in terms of the current density i the correction is:

$$IR = \left(i \cdot 2 r_1 \pi \right) \frac{\rho}{2\pi} \ln (r_2/r_1) = i r_1 \rho \ln (r_2/r_1) \quad (2)$$

For a 3 millimeter spacing, equation (2) becomes:

$$IR = 1.32 i \quad (3)$$

Considering the IR drop to be positive in sign and the measured potential E_m to be negative in sign, the corrected potential of the cathode E_c is:

$$E_c = E_m + (IR) \quad (4)$$

E_m is equal in magnitude to the control potential setting on the potentiostat; therefore, it is evident that the control potential setting must vary with the current density if E_c is to be constant.

This adjustment was made manually as required. Typical overnight variations in current were so small that deviations from the desired control potential were generally less than ± 0.005 volts.

Resistance Measurements. The resistance measurements were made by the potentiometer method (Figure 2). In this method, a specimen is connected in series with a standard resistance R_s and a constant test current is passed through both resistances. The potential E_x across the unknown is compared with the potential E_s across the standard resistance and the resistance of the specimen R_x is calculated from the expression:

$$R_x = \frac{E_x}{E_s} R_s$$

E_x and E_s were measured with a Leeds and Northrup type K3 potentiometer No. 7553-5 and a No. 2430-a galvanometer. R_s was a Rubicon 0.001 ohm standard resistance having a 10 ampere current rating.

A test current of 1.2 amperes was used since this seemed to be a satisfactory compromise between heating effects, which increase with the square of the current, and signal size which is proportional to current. The requirement of a constant test current was obtained by using a 6-volt storage battery with a 5-ohm resistance in series to limit the current flow.

Thermal emfs and the small emf produced by the cathodic protection current flow through the specimen were compensated for by using the galvanometer deflection obtained with the test current off and with the potentiometer set at zero as the null point for the actual measurement.

The temperature of the room was controlled to about $\pm 1^\circ\text{C}$ and the solution temperature was measured on a thermometer graduated in intervals of 0.02°C . The resistance readings were then corrected to 20°C using the expression:

$$R_{20} = \frac{R_T}{1 + \alpha(T - 20)}$$

where T is the temperature of the solution in degrees centigrade, R_T is the resistance of the specimen at a temperature of $T^\circ\text{C}$, R_{20} is the calculated resistance at 20°C and α is the temperature coefficient of resistance. This coefficient can be determined experimentally or it can be calculated from a measurement of the conductivity using the expression:

$$\alpha = \frac{(\text{conductivity in } \% \text{ IACS})}{61.00} \quad 0.00403$$

Both methods gave similar results. Values of 0.00205 and 0.00254 for the -T6 and -T73 tempers respectively were obtained on the specimens used in the present tests.

The results for a typical run are shown in Figure 4. The overall precision of the resistance measurement appeared to be of the order of 0.1% judging from the deviation of values from the best line through the data points. This precision corresponds to an overall error of 0.2 microvolt in measuring E_x .

For very low corrosion rates, the accuracy of the rate measurement becomes directly proportional to the test period. Since something around 400 hours was about the maximum period employed, the uncertainty in a rate measurement would be about ± 0.0005 microhms per hour. The relation between the resistance change and the rate of penetration given in Appendix I indicates

that uniform corrosion producing 0.0005 microhms change per hour is equivalent to a corrosion rate of 0.001 inches per year.

RESULTS:

General. Figure 5 shows the effect of potential on the time to failure of 1/8-inch diameter tensile specimens of 7075-T6 stressed to 75% of the yield strength. As is evident, specimens polarized to potentials less negative than -1.32 v failed by stress corrosion within a few hours; specimens polarized between -1.32 and -1.40 v did not fail and specimens polarized at, or more negative than, -1.40 v failed as a result of alkaline attack from overprotection. The specimen held at -1.325 v showed no sign of stress corrosion even after 400 hours; when tensile tested, it showed only a 2% loss in tensile strength.

Figure 6 shows the effect of potential on the corrosion rate of specimens of 7075-T6 or -T73. For both tempers, the corrosion rate, as measured by the change in resistance, decreased rapidly as cathodic protection was applied. Polarization of 150 millivolts was sufficient to reduce the corrosion rate by a factor of a thousand. Further polarization continued to reduce the corrosion rate until a minimum rate was reached in the vicinity of -1.32 v. Here the rate was too low to measure with precision within the longest exposure period employed, 400 hours. Polarization beyond -1.375 v caused the rate to increase rapidly reflecting overprotection.

The corrosion rates in Figure 6 are the slopes of the corresponding resistance-time curves. The rates were sufficiently similar for both -T6 and -T73 tempers so that it was not necessary to draw separate curves for them. It is to be

emphasized, of course, that similar resistance-time curves do not imply the same corrosive attack. This point is demonstrated by the micrographs in Figure 7 comparing the attack of freely corroding -T73 and -T6 temper specimens. The -T73 temper specimen had the greater weight loss but the attack was more uniform. In the present case, the effects of weight loss and uniformity on resistance evidently tended to compensate.

Effect of Stress. As would be expected, the time to failure of a stressed specimen depended on the stress as well as on the amount of cathodic polarization. This point is illustrated by Figure 8, which compares the effect of four levels of polarization. As is evident, increasing polarization and decreasing stress level both prolonged the time to failure.

All specimens came from the same lot of plate, but they were reheat-treated and aged in batches as the work progressed. Table III summarizes the stress corrosion results in detail in order to show that the variations in stress corrosion performance were not unduly large and also to record all of the data, including some outside the scope of Figures 5 and 8. The data in Table III and Figure 8 indicate that the protective potential range shown in Figure 5 was valid over a considerable range of stress. At the lower stress levels such as 40% and 50% of the yield strength specimens had relatively long lifetimes. Most of the tests were, therefore, conducted at, or above, a stress level of 60% of the yield strength, to avoid tying up a potentiostat for long periods on a single run.

Rate of Stress Corrosion. Data showing the effect of stress on the rate of corrosion of freely corroding specimens are shown in Figure 9; data for specimens polarized to -1.15 v are shown in Figure 10 and data for specimens polarized to -1.25 v are shown in Figure 11.

The accelerating effect of stress is evident in all three figures. In Figure 9 a considerable amount of general corrosion occurred on the unstressed specimen, so that the effect of stress is somewhat less obvious. The cathodic protection levels used in Figures 10 and 11 were sufficient to prevent practically all corrosion in the unstressed specimens. As a result, the resistance change in the stressed specimens is directly related to the progress of the stress corrosion crack. The curves in Figures 10 and 11 suggest two stages in this course.

In the first stage, corrosion proceeded slowly but at a rate which was a function of the stress. When the first stage of corrosion reached a certain level, the rate of change of resistance became more rapid and the resistance began to increase with time in an exponential manner until failure occurred. The data in Figure 10 are replotted in Figure 12 using a logarithmic scale for the change in resistance. The straight line portion of the curves are indicative of a first order rate law (exponential increase). Attention should be directed to the fact that the slope of the straight line portion of a curve is independent of the original stress.

A plot of the logarithm of the resistance change against time for freely corroding specimens stressed at 75 and 60% of the yield strength is shown in Figure 13. The second stage or exponential part of the curve now appears to be followed by a third stage where the slope is considerably smaller. This added complication, compared to the polarized specimens, perhaps reflects the fact that rapid general corrosion is superimposed on the corrosion associated with stress.

Application of Cathodic Protection After Initiation of Stress-Corrosion Cracking. Several experiments were made to determine whether a specimen could be cathodically protected after stress corrosion had started. Specimens were allowed to corrode freely until a given resistance change occurred and then cathodic protection was applied. The results are shown in Figure 14 and in Table IV. Starting with the point of application of cathodic protection, the curve shown in Figure 14 resembles the curve for a specimen polarized to a value somewhat less negative than the protective potential. The explanation appears to be that most of the crack received cathodic protection, but that a small portion was not sufficiently polarized to prevent corrosion. It is not surprising that the throwing power of the electrolyte is limited, especially since the large current densities required for protection would produce correspondingly large IR drops.

Type of Fracturing. In general, conventional metallographic examination with the light microscope proved unsatisfactory for establishing the type of fracturing of the stressed tensile specimens that failed during corrosion. Few of the specimens contained the secondary cracks that usually provide the most conclusive evidence in this type of examination. That they did not reflect the combination of susceptible structure and high stress involved in most instances, and was not unexpected.

The intergranular nature of fracturing over the range in Figure 5 described as "Failure by Stress Corrosion" was demonstrated by electron microscopic examination of replicas of the fractures themselves, as illustrated in Figures 15 - 17. The fracture of every stressed specimen appeared dull with the

exception of a semi-circular region extending in from the outside, which appeared much brighter. As illustrated in Figures 15 - 17, the dull region was transgranular, typical of tensile failure, while the bright region was intergranular, typical of stress corrosion failure.

Little attention was given to establishing the type of fracturing over the range in Figure 5 described as "Failure by Alkaline Attack." Films formed in this range. Because of them, the effective potential at the surface of the metal itself eventually may have become significantly less than the potential applied. The important question about this range was whether alkaline attack occurred; and the curve in Figure 6 showing significant corrosion leaves little doubt that it did.

Metallographic Examination of Cathodically Protected Specimens.

The micrographs at 100X shown in Figure 18 illustrate the effect of cathodic protection on the amount of corrosion. Polarization to -0.90 v greatly reduced the size of the pits, and further polarization to -1.25 v was still more effective. In view of the very small amount of corrosion on the partially protected specimens, it was apparent that a much higher magnification would be helpful and, therefore, oxide replicas from pre-polished specimens subsequently held at various levels of protection were examined by the electron microscope. The technique employed is described briefly in the facing sheet to Figure 19, and results are shown in Figures 19 - 24.

The electron micrographs show that the amount of background etching and the size and frequency of the pits was reduced by cathodic polarization. The behavior of the particles present in the structure can also be observed.

From the electron micrographs, it appears that the potential required to eliminate pitting in unstressed 7075-T6 specimens is identical with the potential required to prevent stress corrosion in the same material.

Although pitting was eliminated at the potential of maximum protection, some slight general etching occurred as can be seen by comparing Figure 24 with the unexposed specimen shown in Figure 19.

Cathodic Protection of Phases. The cathodic protection studies of 7075 alloy were directed toward establishing the phases responsible for stress corrosion. Eventually it was hoped that the phases responsible for stress corrosion could be identified and then reproduced to construct a stress corrosion model. The alloys in Table II were prepared for this purpose, but only a limited amount of attention was given to the evaluation of their electrochemical characteristics.

Solution potential measurements in the electrolyte used for the cathodic protection of 7075 alloy are shown graphically in Figures 25 and 26 for the alloys representing solid solutions on the one hand and equilibrium precipitating phases on the other. Cathodic protection studies were restricted to the most anodic precipitating phase, which corresponded to 100% MgZn_2 . The results are illustrated in Figure 27. The potential required for cathodic protection was not established precisely. The important point is that it appears to be at least in the neighborhood of the potential required for the cathodic protection against stress corrosion of 7075 alloy.

Extraneous Effects. Considerable attention was directed toward establishing that the cathodic protection measurements reflected metallurgical structure rather than extraneous effects such as pH and film formation. Of particular concern was the possibility that the measurements reflected an effect of pH because all the usual cathodic reactions, such as the reduction of hydrogen ion, water or oxygen, tend to increase the pH, and because the resistance to stress corrosion of an aluminum alloy tends to increase as the pH increases.

The results in Figure 28 provide substantial evidence against this possibility. As is evident, the resistance to stress corrosion did improve as the pH increased and very substantially in the neighborhood of pH 10. But all specimens failed by intergranular corrosion as demonstrated by the electron micrographs in Figures 17, 29 and 30. At pH 12, the rate of corrosion was as rapid as that produced by polarization of a specimen to -1.50 v which was well into the range of alkaline attack.

The solution used for the cathodic protection studies was not selected as a result of extensive testing. It was selected because it provided a rate of corrosion that was rapid enough to be measured easily and because it produced stress corrosion quickly. As it turned out, the selection was fortuitous in several respects. Limited tests indicated that, at the very least, cathodic protection was more difficult to obtain without an addition of aluminum chloride; a possible explanation is that the aluminum chloride provided buffering against the development of alkalinity. The data in Figure 31 illustrate an important advantage of a strong acid solution. As

is evident, one effect of raising the pH of the solution was to raise the potential at which cathodic corrosion begins.

A few experiments were made to test the protection provided by the film that gradually developed on a protected specimen. In these tests, specimens were held in the protective range of potential for a considerable period, and then the potential was shifted to a value less negative than the protective potential. The results are shown in Table IV. They indicate only a small effect of any film. For potentials very close to protection, -1.25 or -1.29 v, the pretreatment prolonged the life in two out of four trials, but at -1.15 or -0.75 v the previously protected specimens failed in about the same time as the usual specimens shown in Figures 5 and 8.

Runs where corrosion took place led to contamination of the test solution with the alloying elements of 7075. It was recognized that such contamination, especially by copper ions in solution, might affect the corrosion behavior. The data in Table V show that corrosion products caused some acceleration in stress corrosion but had relatively little effect on the corrosion rate of unstressed specimens.

The depolarizing effect of cupric ions or of the corrosion products of 7075 is evident in the current-time curves in Figure 32. Blanks from 0.250-inch thick plate were used for these measurements. This depolarizing effect made it easy to detect contamination and solutions from a run in which corrosion occurred were not reused. Presumably, copper deposited on the surface of a specimen and provided a cathode surface at which hydrogen reduction proceeded more rapidly. It is interesting to

note in Figure 32 that copper ion added alone was more effective than an addition of the same amount of copper obtained by dissolving 7075. Although the addition of corrosion product made the current requirement to maintain -1.15 v several fold greater than the current requirements to reach a protective potential in uncontaminated solution, the time to failure at -1.15 v remained relatively short indicating that potential rather than current density is the significant factor in cathodic protection.

DISCUSSION:

Without much question, the most significant result of the present investigation is that the stress corrosion of a highly susceptible aluminum alloy in a highly aggressive environment can be prevented by cathodic protection, evidently for an indefinitely long period. Cathodic protection in the present investigation was directed exclusively toward establishing the potential of the most anodic phase involved in the stress corrosion of 7075 alloy. But the fact that it could be achieved in itself is a matter of some consequence. For example, Peterson, Smith and Brown (2) were not able to prevent stress corrosion of 7079-T6 alloy completely in neutral salt solution before overprotection was reached. The value of cathodic protection of aluminum and the difficulties involved have been discussed by several authors (3)(4)(5).

With respect to cathodic protection as a means for establishing the potential of the most anodic phase, the important question naturally is whether this protection reflected microstructural

features or environmental conditions, or both. This question cannot be answered with complete assurance, but there is considerable evidence to support the conclusion that it reflected metallurgical features.

Of most concern initially was the possibility that the protection may have reflected the generation of hydroxyl ions in cathodic reactions; alkalinity generally leads to an improvement in the stress corrosion performance of aluminum alloys. Perhaps the most disturbing argument here is that overprotection began at a potential (and current density) only slightly more negative than that required for cathodic protection against stress corrosion. Strong arguments that the protection did not reflect an effect of alkalinity can be advanced. The most convincing is that the specimens used for the cathodic protection measurements were susceptible to stress corrosion even at a pH as high as 12, although the resistance to corrosion improved somewhat with alkalinity, particularly in the neighborhood of pH 10.

More serious, perhaps is the possibility that cathodic protection may have reflected film formation, at least to some extent. Following this argument, protection would have reflected only the potential at which a film developed. Films did develop on cathodically protected specimens; they could be seen visually. The evidence, however, indicates that they were not appreciably protective; shifting the potential of a specimen from complete to partial protection generally did not increase significantly the time to failure with respect to that of a specimen partially protected only.

The fact that the protective potential in the neighborhood of -1.325 volts was sharply defined in itself suggests that this potential was related to microstructural features and not to extraneous, environmental conditions. Such a potential would be expected from the simple concept of a single anodic phase segregated along a continuous path as a principal factor in stress corrosion.

Also of considerable interest and significance are the results of the resistance measurements in Figures 10 - 11 mapping the course of corrosion and stress corrosion. The results demonstrating an accelerating effect of stress at a very early stage in the corrosion process seem especially significant. They support various theories postulating an electrochemical effect of stress - for example, depolarization of the anodic reaction or a change in anodic potential to a more negative value - that have been advanced from time to time (6)(7). It is informative to consider them briefly in relation to the other results of the investigation.

It is to be emphasized that the microstructural features associated with this so-called strain induced depolarization, to use the terminology of Hoar and others, have not been identified, and that considerable, further work is indicated. Nonetheless, the possibility that the depolarization may be associated with the minute pitting evident in the electron micrographs in Figures 21 - 22 certainly suggests itself. Just how this pitting, apparently associated with constituent, and distributed throughout the matrix, could lead to intergranular corrosion is not clear, but some interaction of pitting and stress

at a grain boundary, would not be unexpected whenever a pit reaches a boundary.

Several observations are relevant to the further development of this possibility. In the first place, the frequency of pitting decreased as the amount of cathodic polarization was increased. In the second place, pitting ceased only when the potential of complete cathodic protection against stress corrosion was reached. And in the third place, the potential of cathodic protection against stress corrosion was the potential where the corrosion rate was a minimum, as shown in Figure 6, as well as the potential where pitting ceased. These observations, it would seem, are consistent with the fact that the time to failure of a stressed specimen increased progressively as the potential of cathodic protection became more negative until, at the potential of complete protection, it became infinitely long.

The curves in Figures 10 - 12 mapping the course of stress corrosion reveal even more about the second stage of this process, which began an hour or so before a specimen failed, than they do about the first stage. For the same potential, the corrosion process in this second stage was the same for all specimens, independently of the original stress applied to them as is indicated by the fact that the corrosion followed the same exponential or first order rate in each case. The original stress did affect the corrosion required for the second stage to develop. Figure 12 indicates qualitatively that more corrosion was required, the lower the original stress. The meager evidence suggests that the second stage developed when the stress on the uncorroded portions of every specimen reached the same value. Intuitively, one suspects that this value corresponds to the

yield strength. Some support of this viewpoint is provided by the fact that, for the specimens in Figure 12, a roughly linear relation was obtained by plotting the change in resistance required for the initiation of the second stage against the calculated decrease in cross sectional area required to produce a stress equal to the yield strength. A considerable effect of yielding upon depolarization would be expected (6).

A comparison of Figures 10 and 11 indicates that the rate of the second stage was less the more negative the potential. With all conditions the same, the polarization of the tip of a crack would be expected to be greater, and the rate of corrosion correspondingly less, the more negative the applied potential.

The rate equation for the second stage can be written in either an integral or a differential form as follows:

$$\Delta R = k e^t \quad \text{or} \quad \frac{d(\Delta R)}{dt} = k_1 \Delta R$$

Where ΔR is the change in resistance and t is the time. The differential form indicates that the rate of change in resistance is a function of the resistance change. A possible physical picture is that the rate of growth of a crack at this stage is a function of the size of the crack, or alternately of the length of the tip of the crack. An important implication of the expression is that the final stage of the stress corrosion process is limited, not by the applied stress, but by some other factor. Diffusion immediately suggests itself as a possibility to be explored.

Relatively gross pitting, as revealed at a magnification of 100X, stopped by the time cathodic protection had reached a

potential as negative as -0.95 to -1.00 v. At one time in the investigation, the evidence seemed to suggest that the potential at which this gross pitting stopped corresponded to a critical potential advanced by Kologyrkin (8). The more complete evidence now available does not seem to suggest the theory of a critical potential nearly so well. For one thing, gross pitting stopped, not at a well defined potential, but rather over a range of potential. There was no evidence, however, that the gross pitting had any bearing on the stress corrosion process and for this reason its possible relation to the theory proposed by Kolotyrkin was not explored in depth.

One final point perhaps should be discussed briefly. At first glance, the fact that a minute amount of corrosion occurred at the potential of cathodic protection against stress corrosion may seem disconcerting. If so, it should be recalled that absolute cessation of corrosion in a thermodynamic sense is expected only when a metal and its ions are in true equilibrium (9), and this condition is unlikely with aluminum. The important point is that corrosion of the phases involved in the stress corrosion process was prevented.

* * *

To summarize: The present investigation demonstrates some interesting and significant aspects of the stress corrosion of aluminum alloys. But more important, perhaps, it has led to the development of experimental techniques and pointed the way for further investigation of this process. Further work to establish the course of stress corrosion at various levels of cathodic

protection, in various electrolytes, and to relate this course to microstructural features, especially as revealed with the electron microscope, should be particularly profitable.

References

- (1) G. L. Booman, Analytical Chemistry 29, 213-218 (1957).
- (2) M. H. Peterson, J. A. Smith, B. F. Brown, "Effects of Electrochemical Potential of Stress-Corrosion Cracking of Aluminum Alloy 7079-T6 in Salt Water". Paper presented at the Second International Congress on Metallic Corrosion, New York, New York, March 1963.
- (3) W. J. Schwerdtfeger, Journal of Research of the National Bureau of Standards 68C, 283-294 (1964).
- (4) J. F. Whiting and T. E. Wright, Corrosion 17, 8, (1961).
- (5) R. H. Brown, Conference Paper Presented at the 30th Spring Meeting of the American Society of Refrigerating Engineers, Cleveland, Ohio, June 1, 1943.
- (6) T. P. Hoar, Corrosion 19, 331 t (1963).
- (7) R. N. Parkins, Metallurgical Reviews, 9, No. 35, 201-260 (1964).
- (8) J. M. Kolotyrkin, Journal of the Electrochemical Society 108, 209-216.
- (9) E. Deltombe and M. Pourbaix, Corrosion 14, 496 t, (1958).

TABLE I
CHEMICAL ANALYSIS AND PROPERTIES OF TWO-INCH THICK
7075-T6 AND -T73 ALLOY PLATE

Chemical Analysis of Plate									
<u>Cu</u>	<u>Fe</u>	<u>Si</u>	<u>Mg</u>	<u>Mn</u>	<u>Zn</u>	<u>Ni</u>	<u>Cr</u>	<u>Ti</u>	<u>Be</u>
1.62	0.20	0.09	2.63	0.04	5.92	0.00	0.17	0.02	0.001

Tensile Properties in Short-Transverse Direction and Electrical
Conductivities

<u>Temper</u>	<u>T.S. psi</u>	<u>Y.S. psi</u>	<u>El. % in 0.5"</u>	<u>Conductivity % IACS</u>
-T6	82,400	74,600	2.0	31.0
-T73	71,500	65,800	2.9	38.5

Note: Blanks (1/4" x 1/4" x 2") taken in the short-transverse direction from two-inch thick 7075-T651 alloy plate (S-274086) were reheat treated one hour at 870°F, quenched in cold water and then artificially aged to the -T6 and -T73 tempers.

TABLE II

ALLOYS PREPARED TO DUPLICATE SOLID SOLUTION AND PRE-
CIPITATING PHASES IN 7075 ALLOY

S. - No.	Description	Composition					
		Al	Cu	Mg	Zn	Cr	Be
<u>Solid Solution Alloys</u>							
292861	Nominal Cu, 3/4 Nominal Mg, Zn	----	1.60	2.00	4.50	0.20	0.002
862	Nominal Cu, 1/2 Nominal Mg, Zn	----	1.60	1.25	2.75	0.20	0.002
863	Nominal Cu, 1/5 Nominal Mg, Zn	----	1.60	0.50	1.00	0.20	0.002
864	1/2 Nominal Cu, 3/4 Nominal Mg, Zn	----	0.80	2.00	4.50	0.20	0.002
865	1/2 Nominal Cu, 1/2 Nominal Mg, Zn	----	0.80	1.25	2.75	0.20	0.002
866	1/2 Nominal Cu, 1/5 Nominal Mg, Zn	----	0.80	0.50	1.00	0.20	0.002
<u>Precipitating M-Phase Alloys</u>							
292647	100% MgZn ₂ , 0% CuMgAl	----	----	15.70	84.30	----	0.02
648	80% MgZn ₂ , 20% CuMgAl	4.70	11.10	16.80	67.40	----	0.02
649	60% MgZn ₂ , 40% CuMgAl	9.40	22.10	18.00	50.50	----	0.02
650	40% MgZn ₂ , 60% CuMgAl	14.10	33.20	19.00	33.70	----	0.02

TABLE III

SUMMARY OF DATA RELATING TIME TO FAILURE, STRESS
LEVEL AND POTENTIAL

<u>S. No.</u>	<u>Potential, MV - SCE (a) (c)</u>	<u>Failure Time, Hours (b)</u>
<u>Stressed to 40% Yield Strength</u>		
320713-N20	-750	6.85
320713-N19	-750	10.2
<u>Stressed to 50% Yield Strength</u>		
320713-N17	-750	4.87
320831-N1	-1000	37.8
320831-N2	-1150	10.5
<u>Stressed to 60% Yield Strength</u>		
320713-N12	-750	2.4
320713-N10	-1150	4.0
320831-N38	-1150	6.43
320713-N9	-1250	34
320831-N39	-1250	46.4
320713-N13	-1325	OK 113
320713-N13	(-1290*)	OK 170
320713-N13	(-1250*)	OK 167
320713-N13	(-750*)	3.3
<u>Stressed to 75% Yield Strength</u>		
311752-N4	-750	0.5
320413-N28	-750	0.97
320413-N44	-750	1.17
320413-N40	-750	1.33
320831-N17	-750	2.42
320209-N9	-760	3.0
320209-N13	-900	2.4
320831-N16	-1150	4.2
320209-N14	-1150	5
320413-N2	-1250	14.7
320831-N21	-1250	39.5
320413-N31	-1290	0.5
320413-N3	-1325	OK 399
320413-N32	-1325	OK 17
320413-N32	(-1290*)	11.8
320413-N9	-1375	OK 305
320413-N9	(-1150*)	4.28
320413-N8	-1450	48.5
320413-N33	-1450	202
320413-N5	-1510	29
320413-N7	-1550	17
<u>Stressed to 90% Yield Strength</u>		
320713-N22	-750	1.18
320713-N23	-1308	29.2
320713-N25	-1325	OK 92
320713-N25	(-1290*)	OK 77
320713-N25	(-1150*)	0.36
320713-N24	-1365	OK 164
320713-N24	-1290	15.6
320713-N26	-1400	109

(Continued)

TABLE III
(Continued)

- Notes: (a) An asterisk on the potential value is used to indicate that the specimen was initially polarized to the more negative potential shown by the preceeding entry.
- (b) "OK" designation indicates failure did not occur.
- (c) The corrosion potential of 7075-T6 was -750 mv SCE, and all of the entries at this potential are for freely corroding specimens.

TABLE IV

APPLICATION OF CATHODIC PROTECTION, FOLLOWING A PERIOD
OF FREE CORROSION. 7075-T6 SPECIMENS STRESSED TO 75%
OF THE YIELD STRENGTH

<u>S. - No.</u>	<u>Free Corrosion</u>		<u>Cathodic Polarization</u>	
	<u>Time</u> <u>Min</u>	<u>ΔR</u> <u>Microhms</u>	<u>Potential</u> <u>V. SCE</u>	<u>Total</u> <u>Time to</u> <u>Fail, Hour</u>
320713-N1	70	1.50	-1.325	14
320413-N45	48	1.20	-1.390	7.7
320413-N41	42	0.80	-1.450	9.1

TABLE V

EFFECT OF PRIOR EXPOSURE AT A PROTECTIVE POTENTIAL
ON THE TIME TO FAILURE IN SUBSEQUENT EXPOSURE AT
LESS NEGATIVE POTENTIALS EACH SPECIMEN WAS EXPOSED
AT SUCCESSIVELY LESS NEGATIVE POTENTIAL UNTIL FAILURE
OCCURRED

<u>S. - No.</u>	<u>Stress % Y. S.</u>	<u>Time to Failure, Hours</u> (Potential, Volts vs SCE)					
		<u>-1.36 v</u>	<u>-1.32 v</u>	<u>-1.29 v</u>	<u>-1.25 v</u>	<u>-1.15 v</u>	<u>-0.75v</u>
320713-N25	90	OK/69	OK/23	OK/77		F/0.3	
320713-N24	90	OK/164		F/15.6			
320413-N9	75	OK/305				F/4.3	
320413-N32	75		OK/17	F/11.8			
320713-N13	60		OK/113	OK/168	OK/167		F/3.0

TABLE VI

EFFECT OF DISSOLVED CORROSION PRODUCT ON THE
CORROSION AND STRESS CORROSION OF 7075-T6

<u>Solution (a)</u>	<u>Potential, Volts S.C.E.</u>	<u>Stress Level, % Yield Strength</u>	<u>Time to Failure, Hours</u>	<u>Corrosion Rate microhms/hr.</u>
Fresh	Free corrosion (-0.75)	Unstressed	--	2.4
Fresh + 5 ppm Cu	Free corrosion (-0.75)	Unstressed	--	2.6
Fresh	Free corrosion (-0.75)	75	1.4, 1.0	
Old (5 ppm Cu) (b) (c)	Free Corrosion (-0.75)	75	0.5	
Fresh	-1.15	75	5.0, 4.3	
Fresh + 5 ppm Cu (c)	-1.15	75	2.9	
Fresh + 25 ppm Cu (c)	-1.15	75	3.2, 1.3	

Notes: (a) The electrolyte contained 1 mole/liter NaCl, 0.2 mole/liter AlCl₃, with the pH adjusted to 1 with HCl.

(b) Estimated by qualitative spectrographic analysis and polarization tests.

(c) The copper content was obtained by dissolving the appropriate amount of 7075.

Figure 1

Diagram of apparatus for cathodic protection experiments.

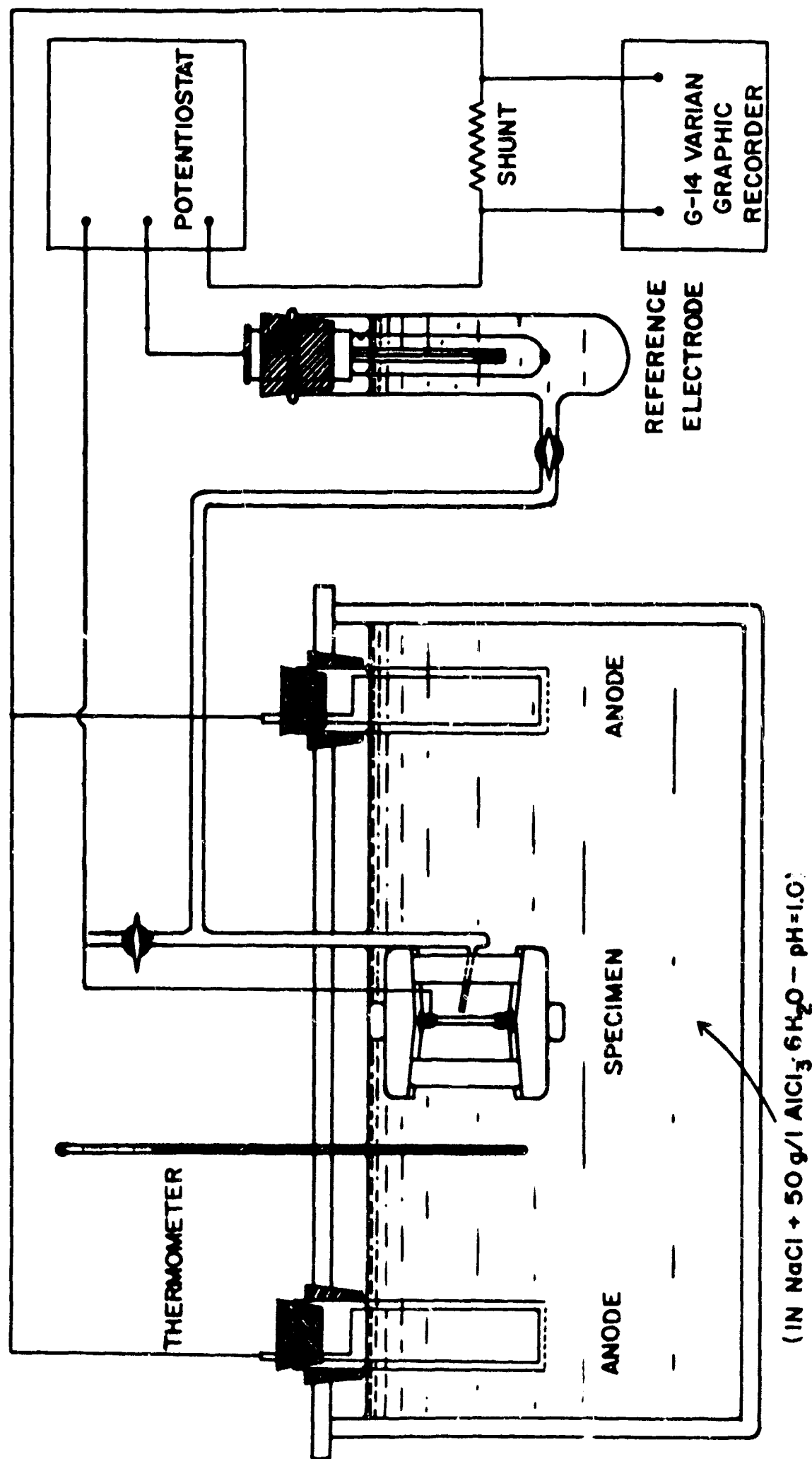


Fig. 1

Figure 2

Diagram of circuit for measuring the electrical
resistance and the time to failure of a specimen.

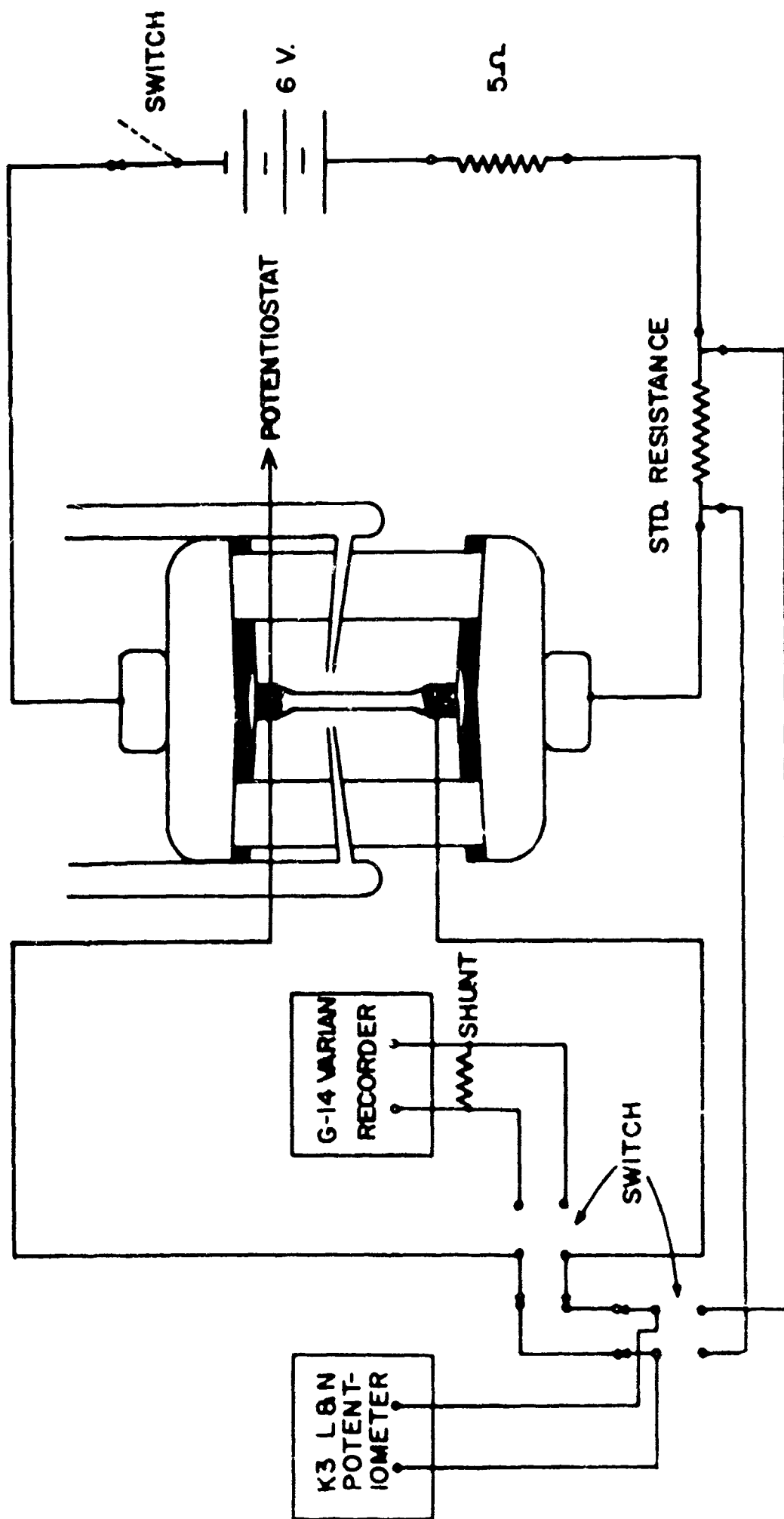


Fig. 2

Figure 3

Photographs of stressed specimens showing percussion welded connections (A), Luggin capillaries (B) and wax coating (C).

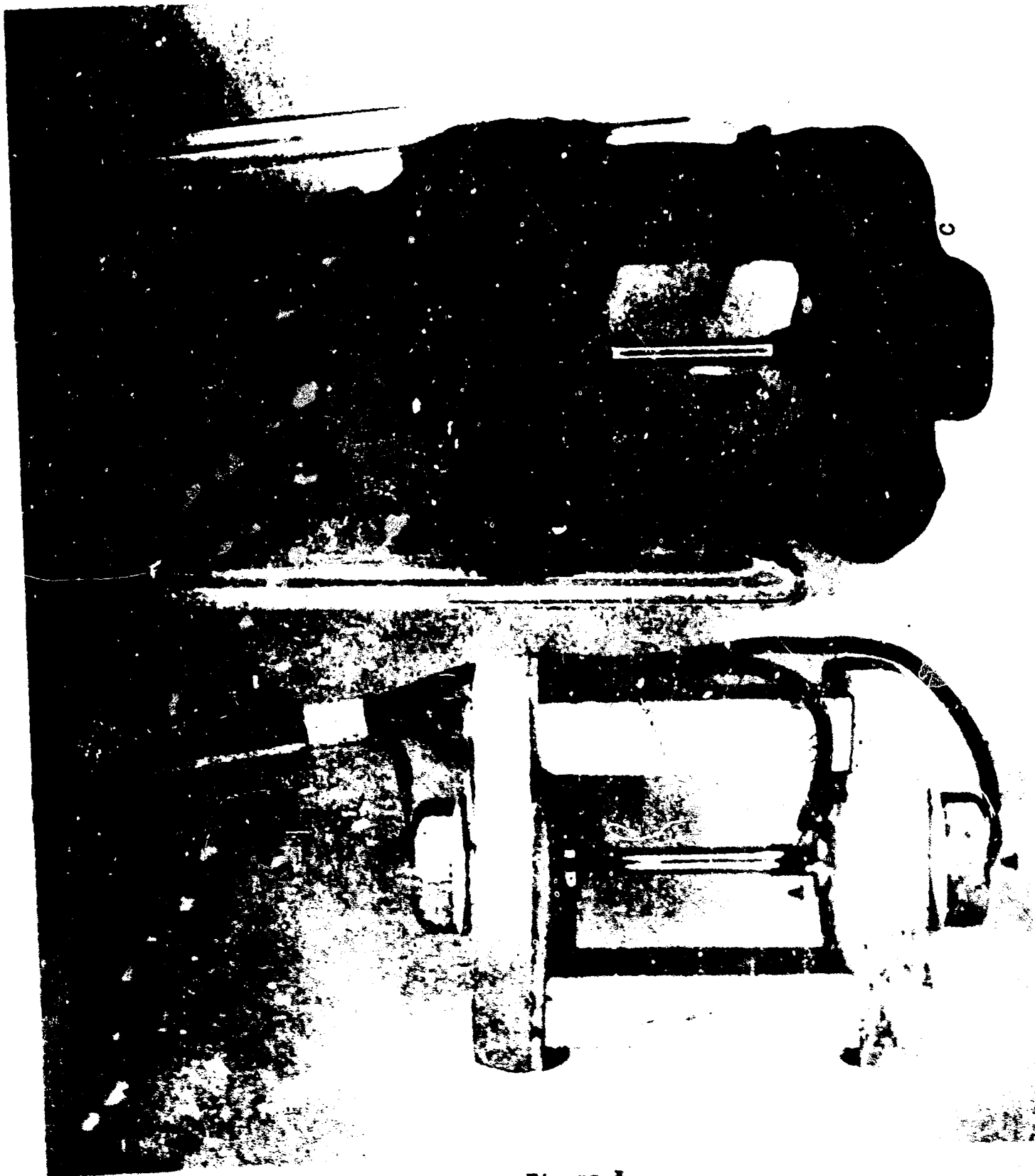
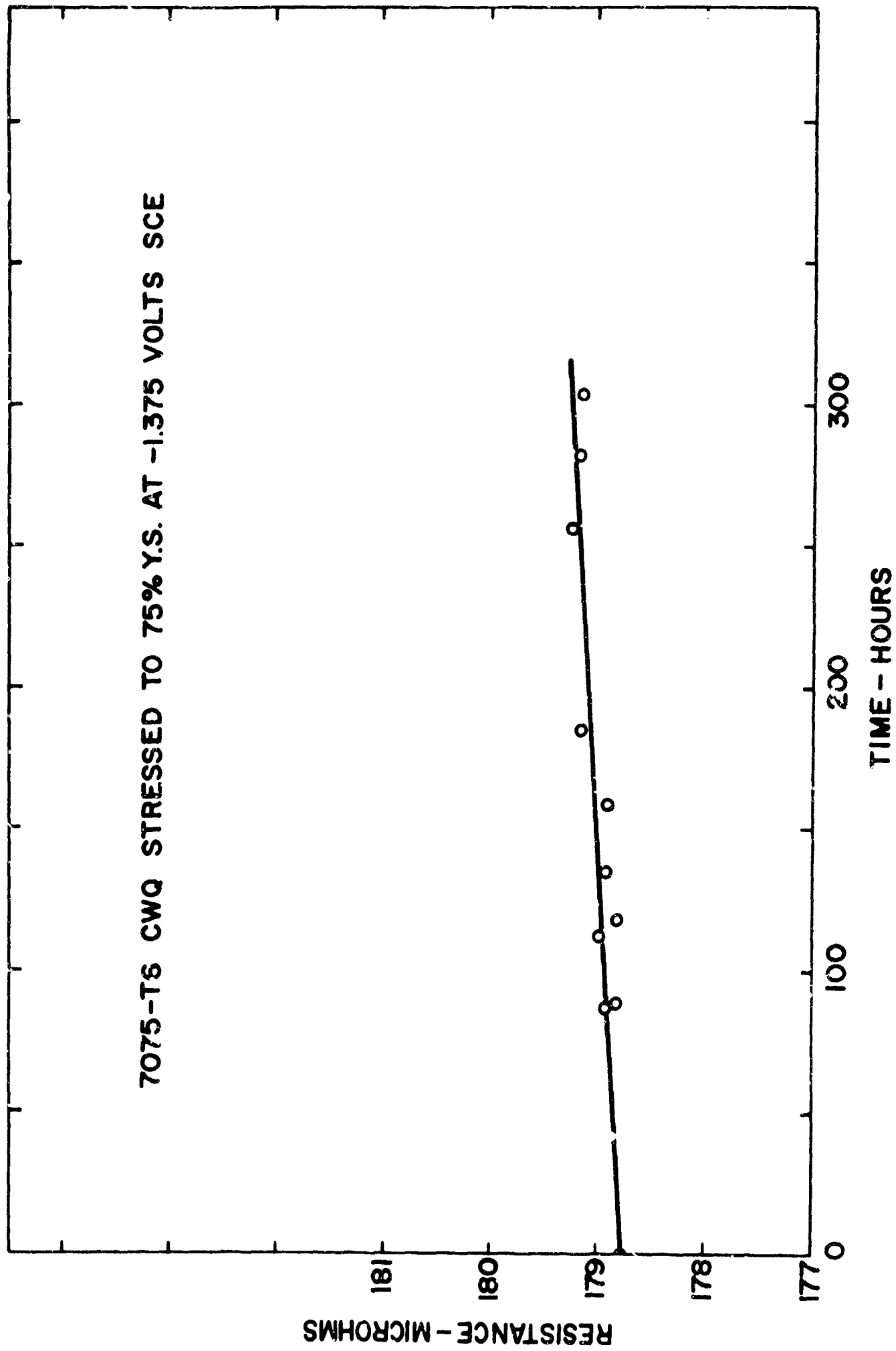


Figure 3

Figure 4

A typical resistance vs. time plot illustrating the spread of experimental readings.



49

Figure 5

Effect of applied cathodic potential on the stress corrosion performance of stressed short-transverse specimens from 7075-T6 alloy plate.

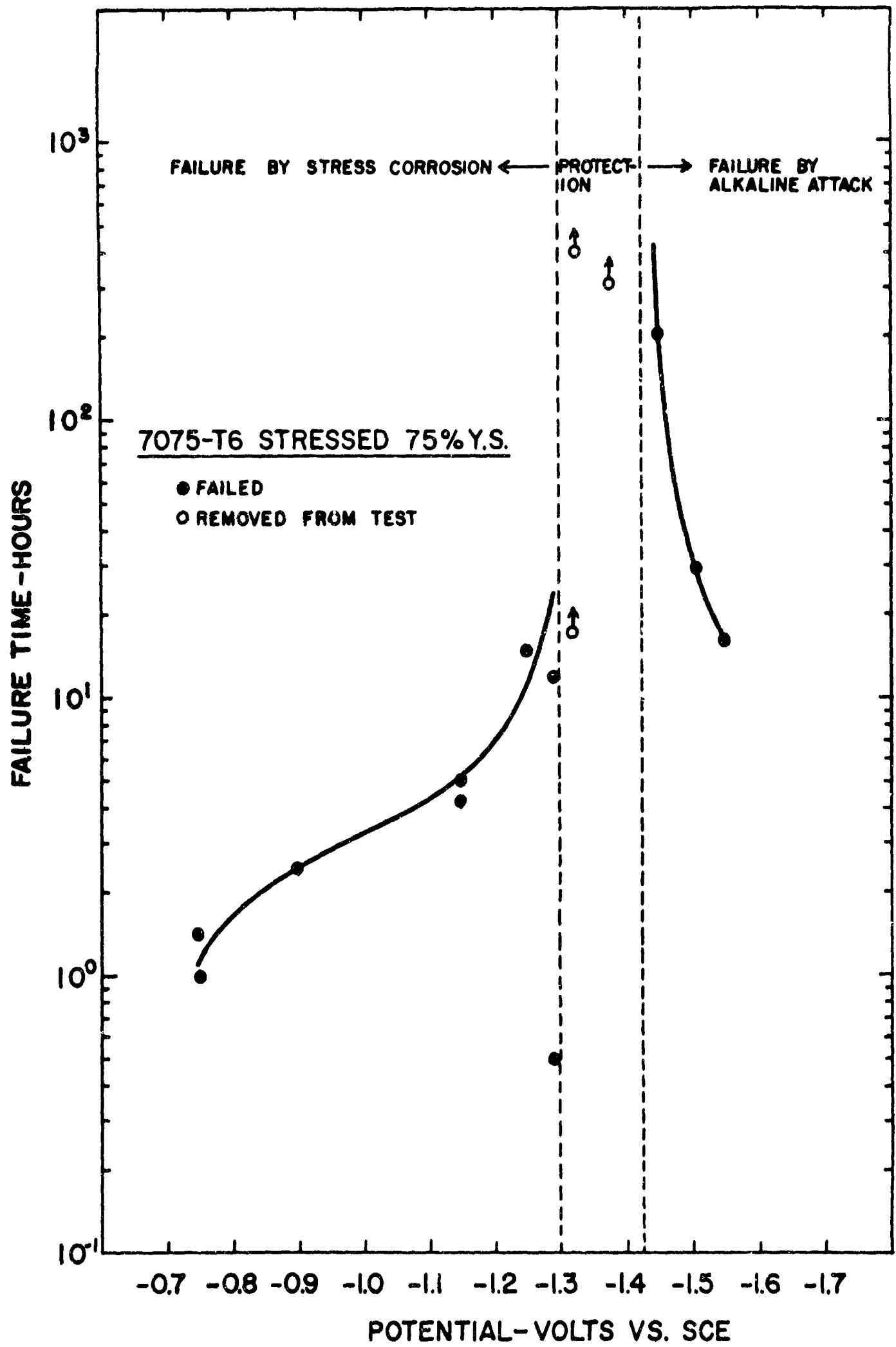


Fig. 5

Figure 6

Effect of applied cathodic protection on the corrosion rate of short transverse specimens from 7075-T6 and -T73 alloy plate. The points include both unstressed and stressed specimens; with the exception that stressed -T6 specimens in the potential range from -0.8 to -1.3 volts have not been included because the effect of stress was appreciable in this range. In the vicinity of the minimum rate the curves have been dashed, because the rate is too low to measure with precision within the longest exposure period employed, 400 hours.

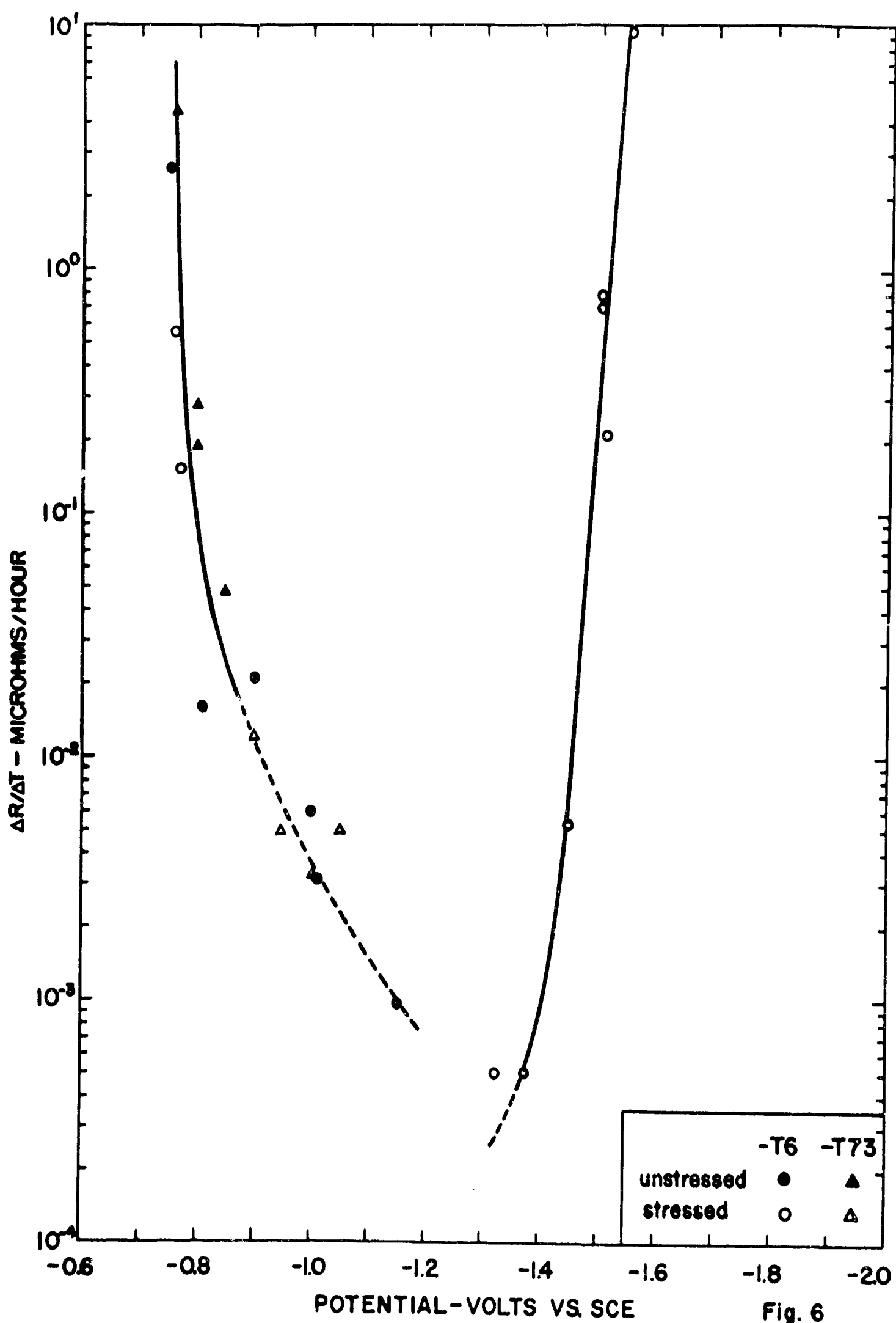


Fig. 6

Figure 7

Micrographs of sections through freely corroding
7075-T6 and -T73 specimens.



7075-T6 UNSTRESSED

22 HOURS



7075-T73 UNSTRESSED

38 HOURS

KELLER'S ETCH

MAGNIFICATION 100X

**SECTIONS OF 1/8" DIAMETER SHORT TRANSVERSE
TENSILE SPECIMENS AFTER FREE CORROSION
IN ACIDIFIED $\text{NaCl}/\text{AlCl}_3$ SOLUTION**

Figure 7

Figure 8

Effect of stress level on time to failure of 7075-T6 specimens for several levels of polarization. The solid lines indicate the range of data for each level of polarization.

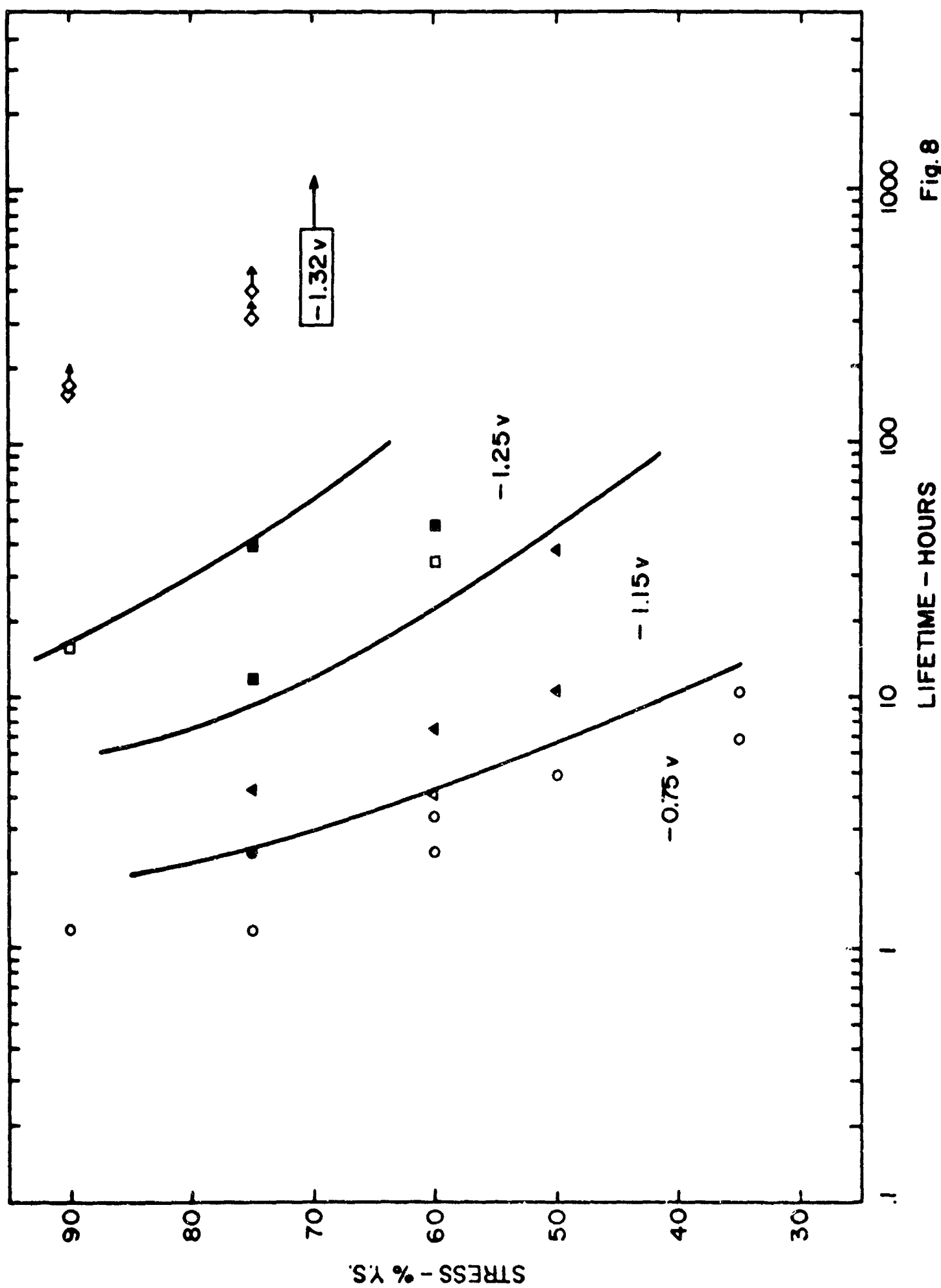


Fig. 8

Figure 9

Resistance vs. time plots for freely corroding specimens illustrating the effect of stress.

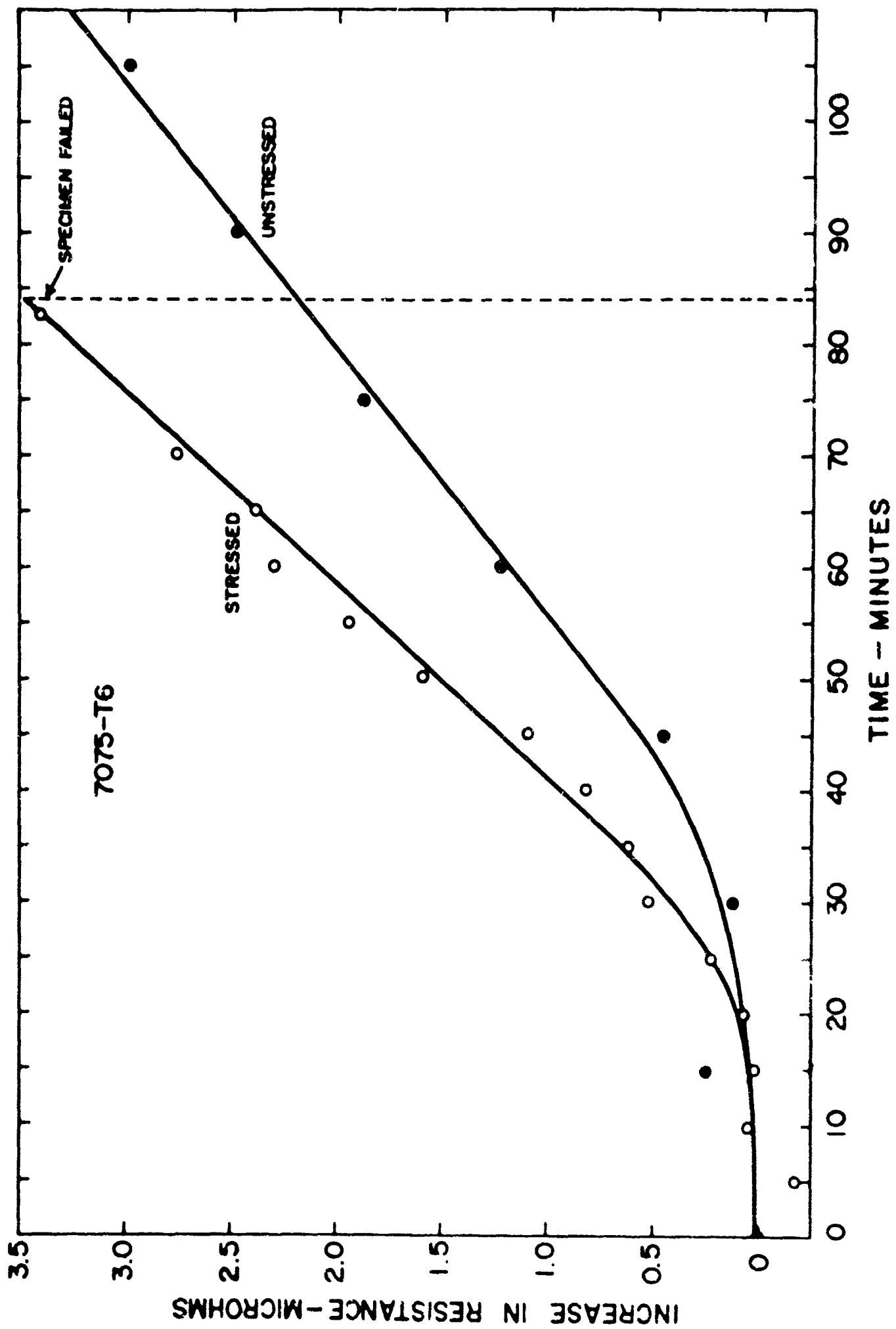


Fig. 9

Figure 10

Data showing the effect of stress level on the resistance vs time curves. The specimens are 7075-T6 polarized to -1.15 v.

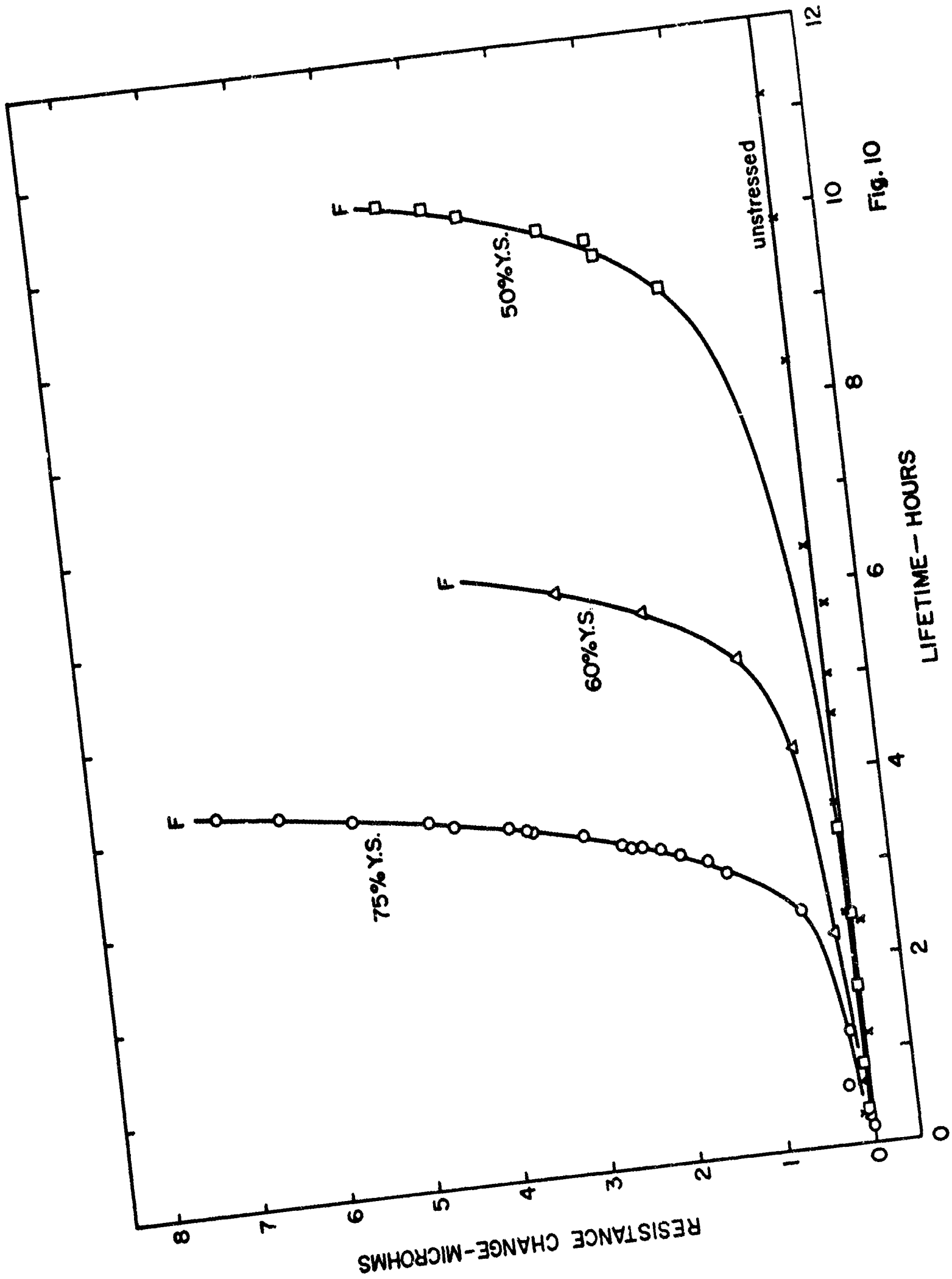


Fig. 10

Figure 11

Data showing the effect of stress level on the resistance vs time curves. The specimens are 7075-T6 polarized to -1.25 v.

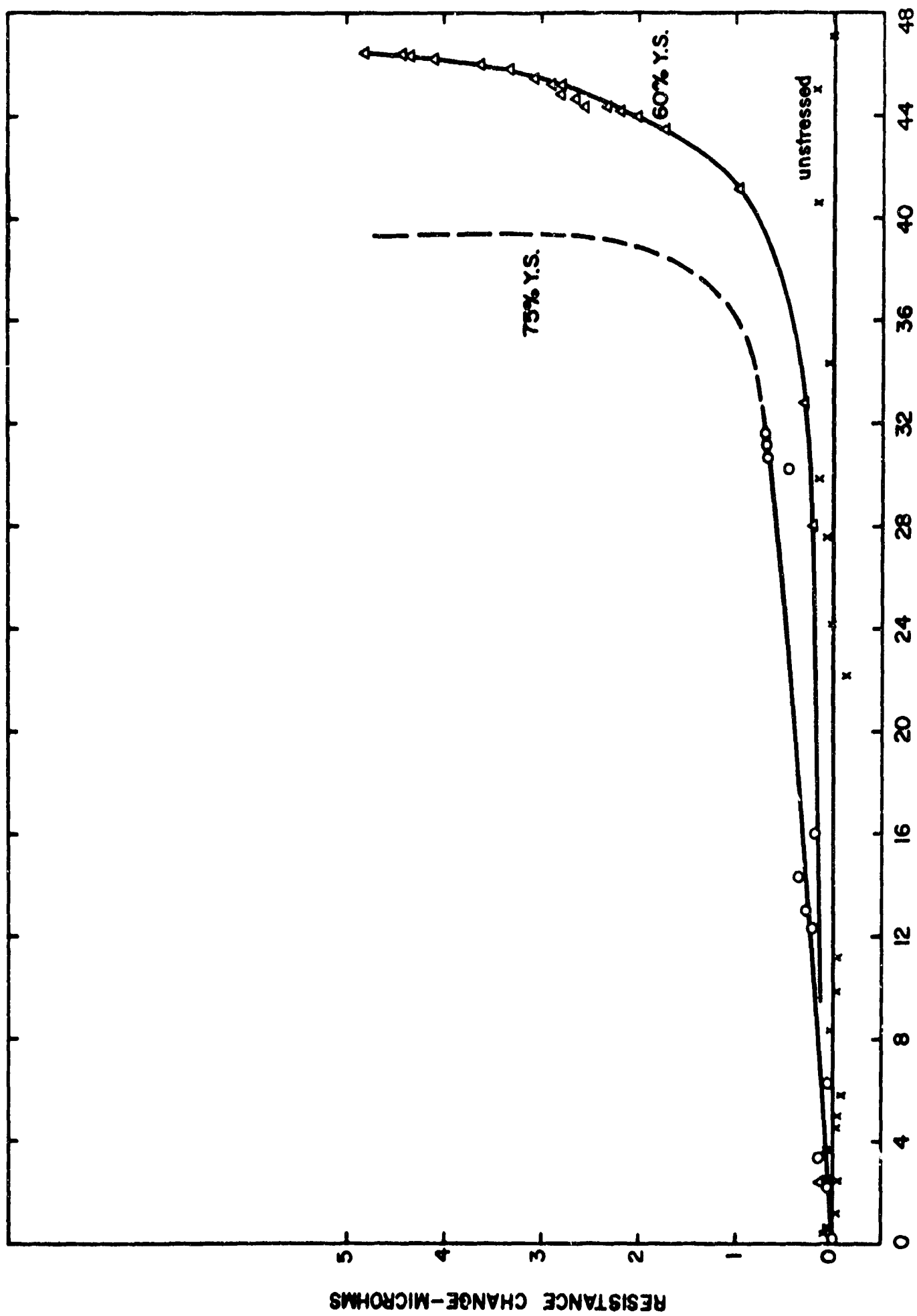


Fig. II

Figure 12

A replot of the data in Figure 10 using a logarithmic scale for resistance change in order to illustrate the exponential resistance increase immediately preceding the failure. The specimens are 7075-T6 polarized to -1.15 v.

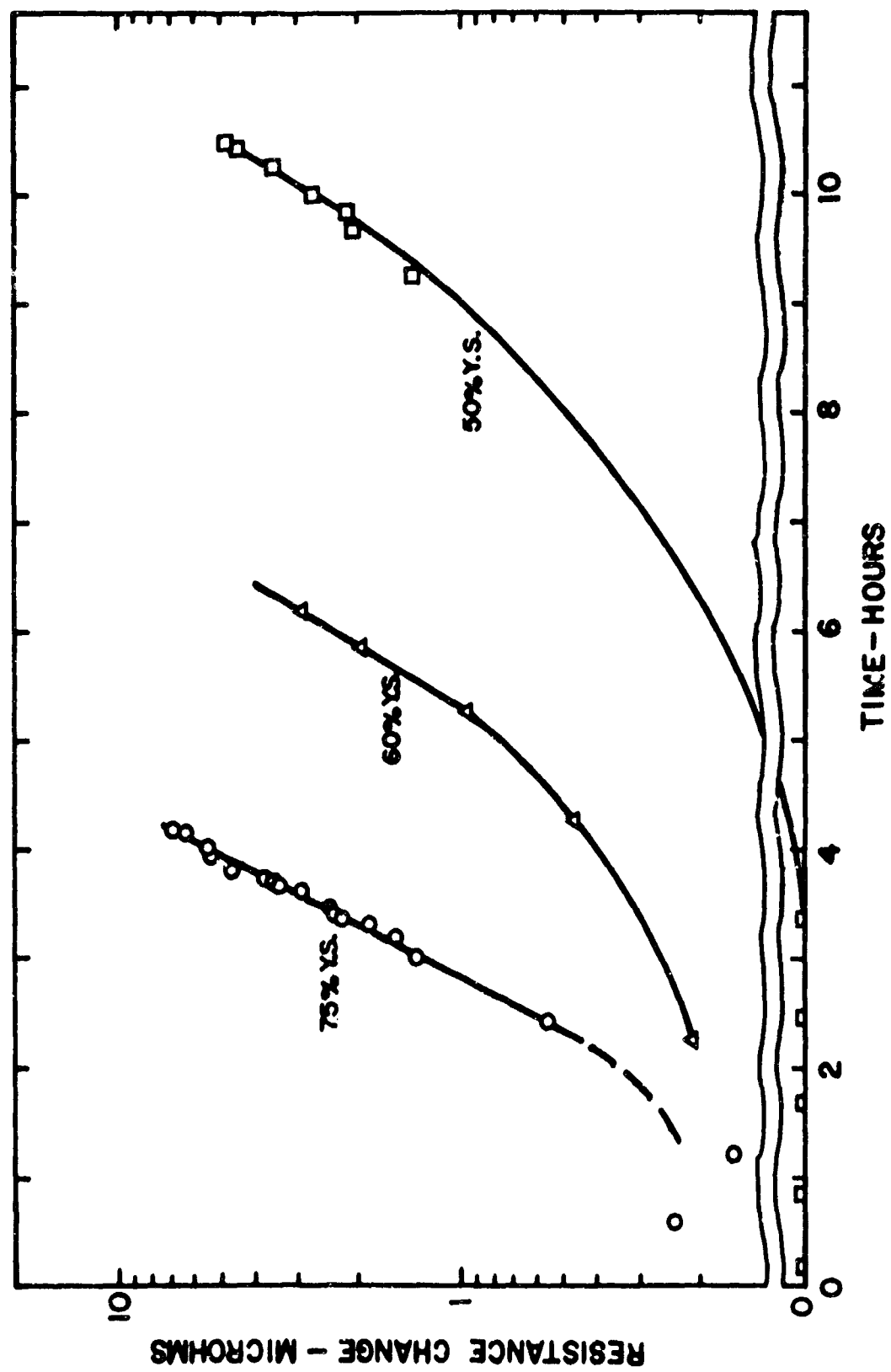


Fig. 12

Figure 13

Semi-logarithmic plot of resistance change vs time for freely corroding specimens of 7075-T6. In contrast to polarized specimens shown in Figure 12, the exponential part of the curve now shows two branches.

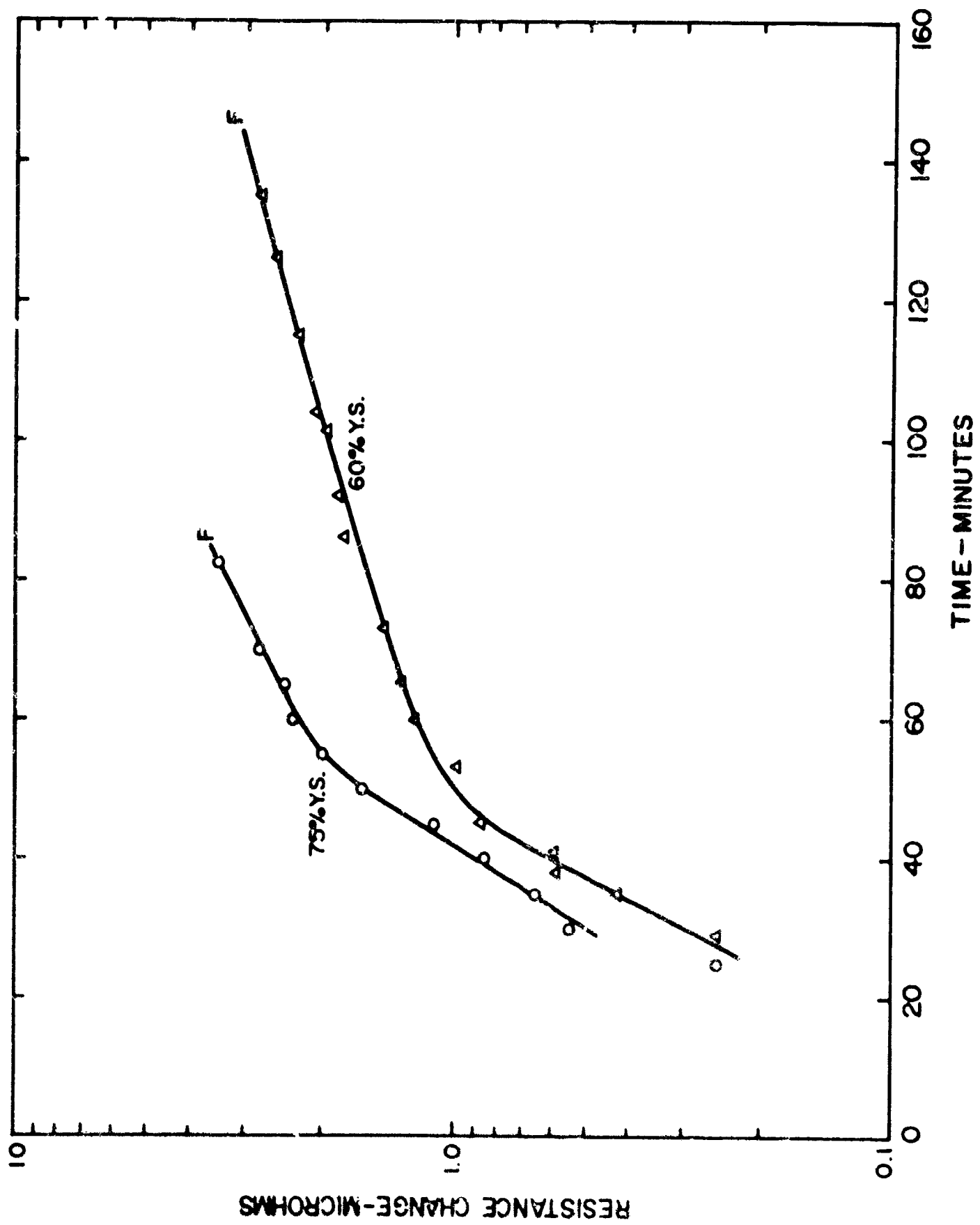


Fig. 13

Figure 14

Effect of cathodic protection applied to 7075-T6 after a period of free corrosion. The scatter in the data is larger than normal, and is attributed to parasitic thermal emfs which were eliminated in all other experiments.

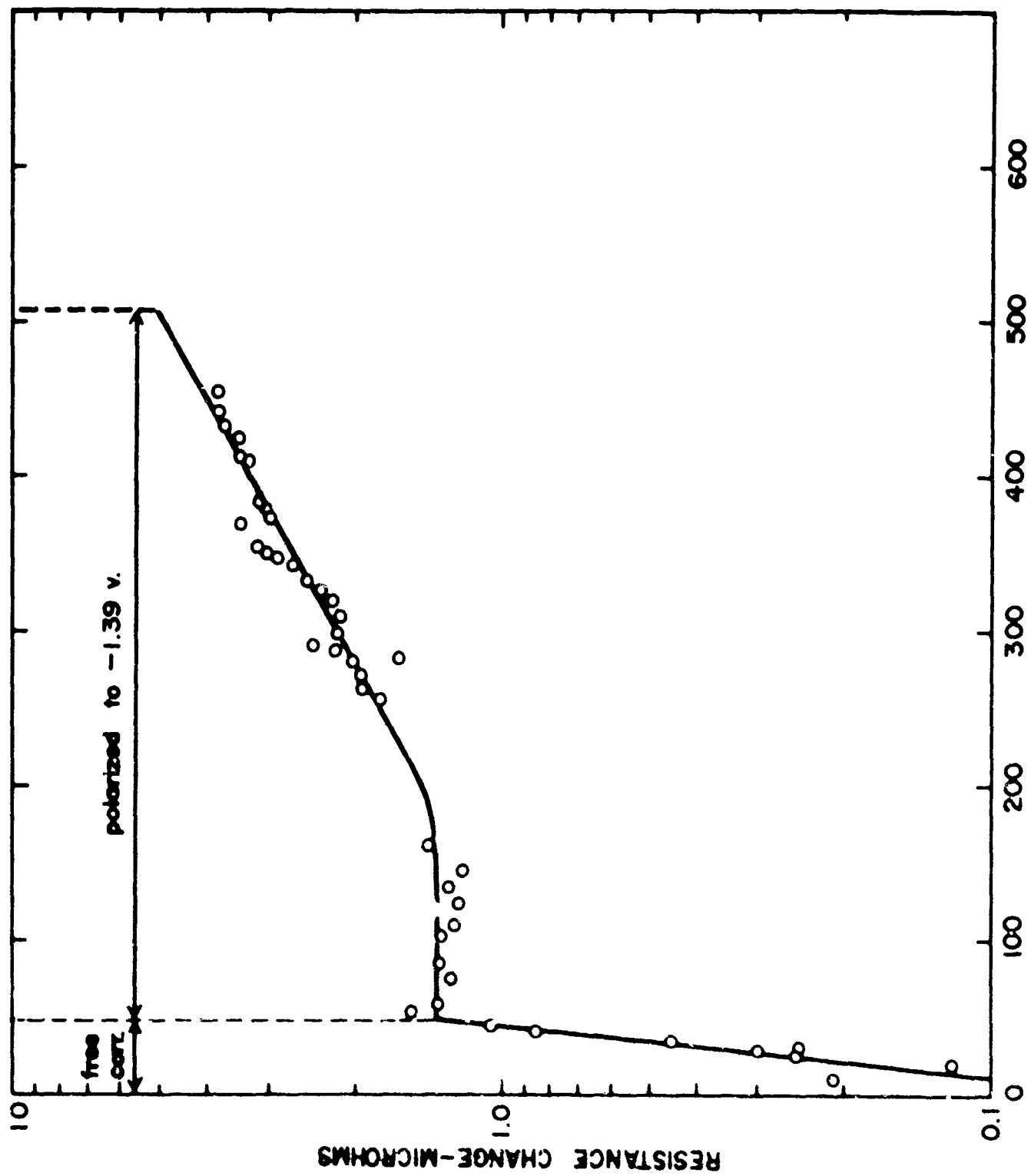
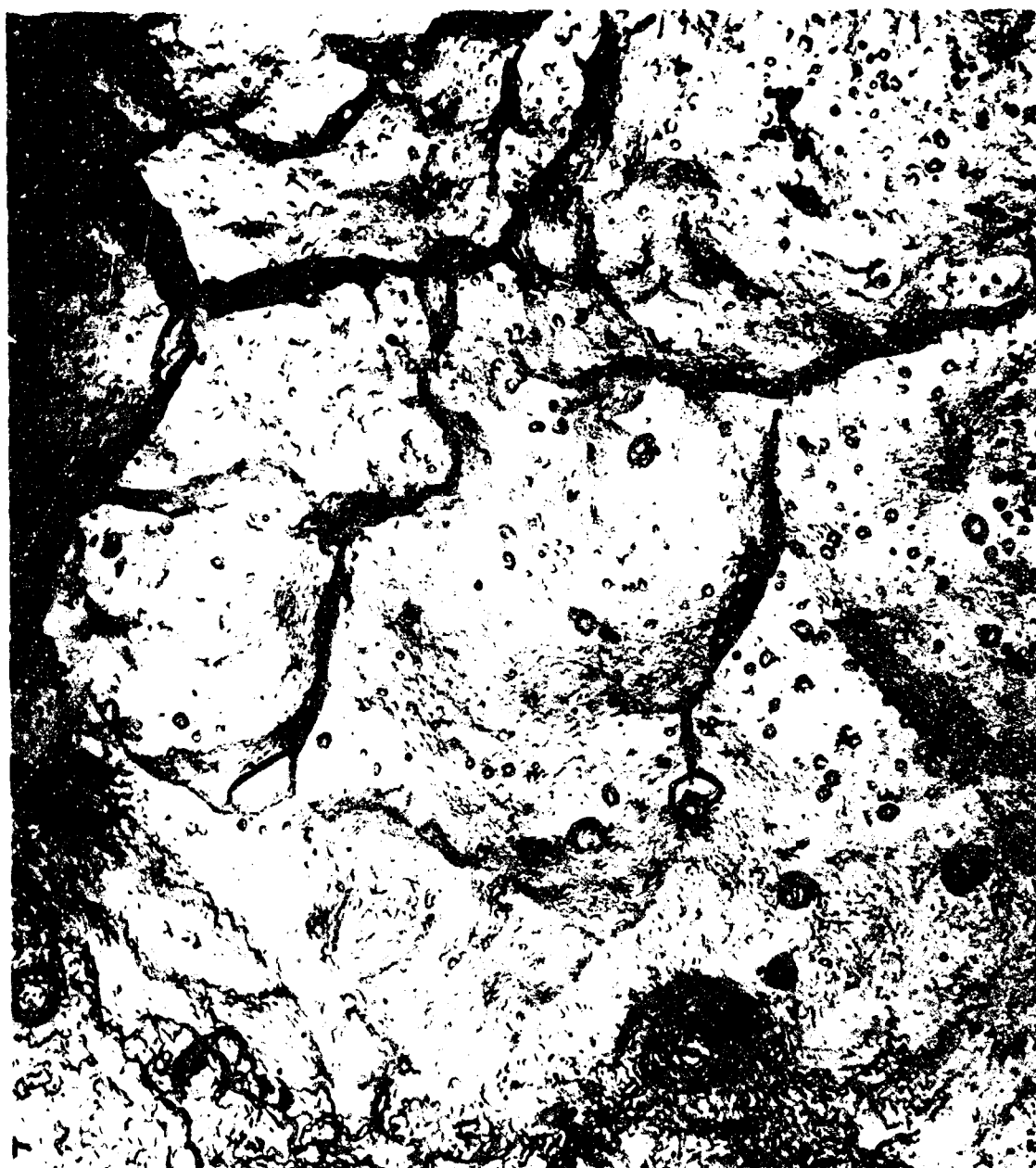


Fig. 14

Figure 15

Electron micrograph showing the intergranular nature of the bright portion of a fracture. 7075-T6 specimen stressed to 75% of the yield strength, and polarized to -1.29 volts; failed after 11.8 hours.



320413-N32

Oxide Replica

5,000X

Figure 15

Figure 16

Electron micrograph showing the transgranular nature of the dull portion of a fracture. Same specimen shown in Figure 15.



320413-N32

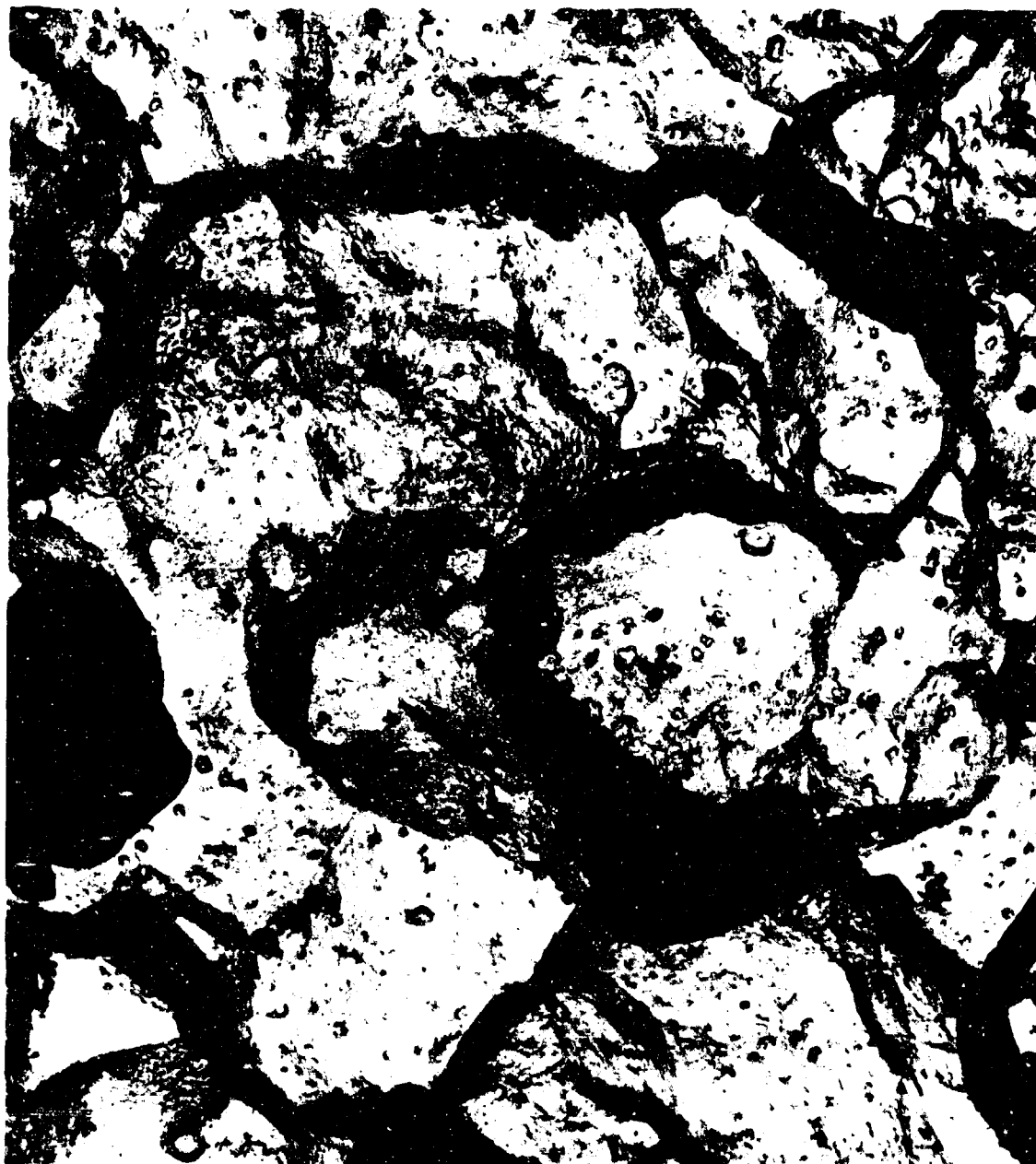
Oxide Replica

5,000X

Figure 16

Figure 17

Electron micrograph showing intergranular nature of the bright portion of a fracture. 7075-T6 specimen stressed to 75% of the yield strength and exposed to free corrosion.



320413-N44

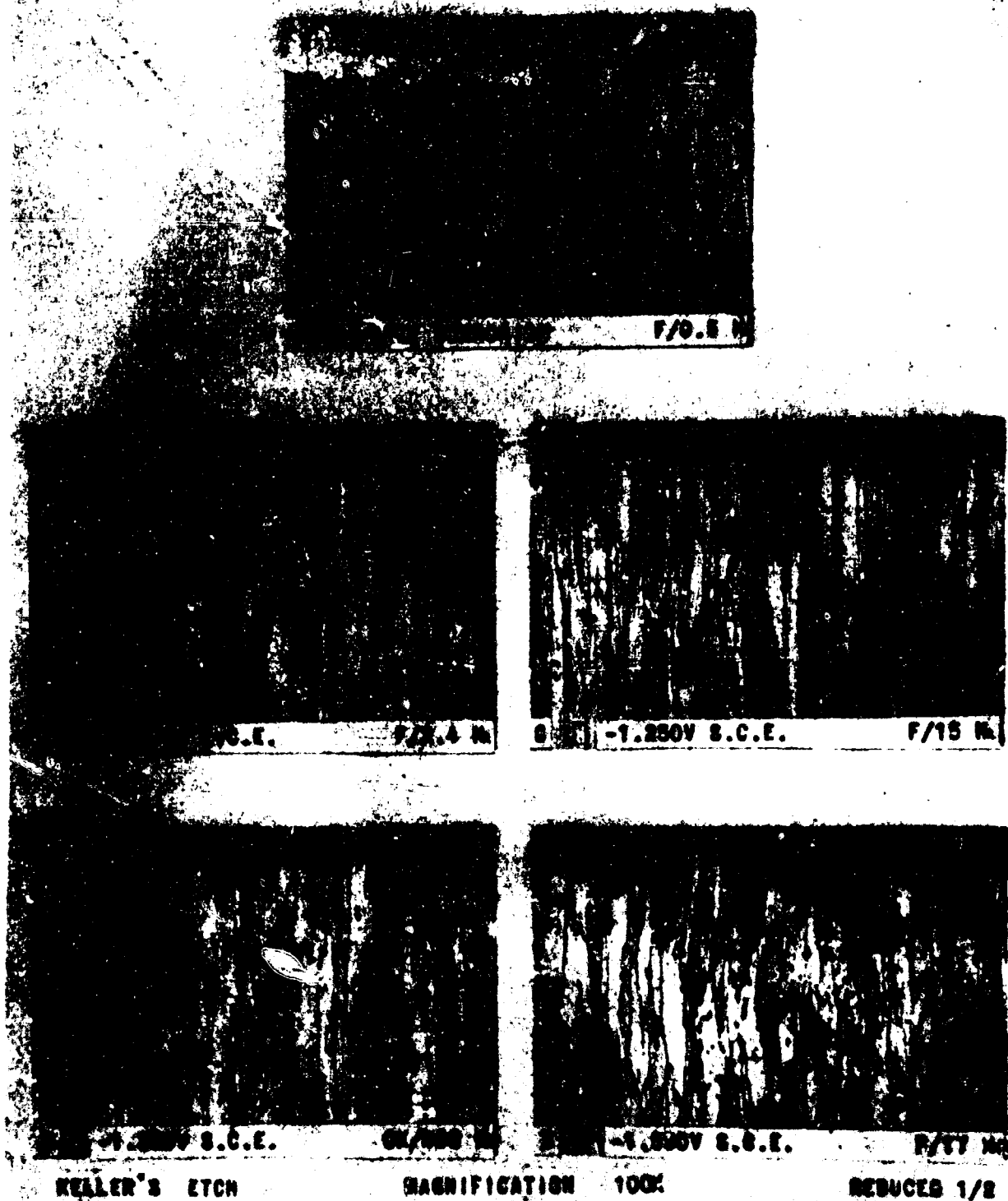
Oxide Replica

5,000X

Figure 17

Figure 18

Micrographs of sections through stressed 7075-T6 specimens cathodically protected at various potentials. Note the stress-corrosion crack in "A" indicated by an arrow and the small pits in "B" also indicated by arrows. Pitting could not be detected in "C" or "D". The pitting in "E" resulted from overprotection.



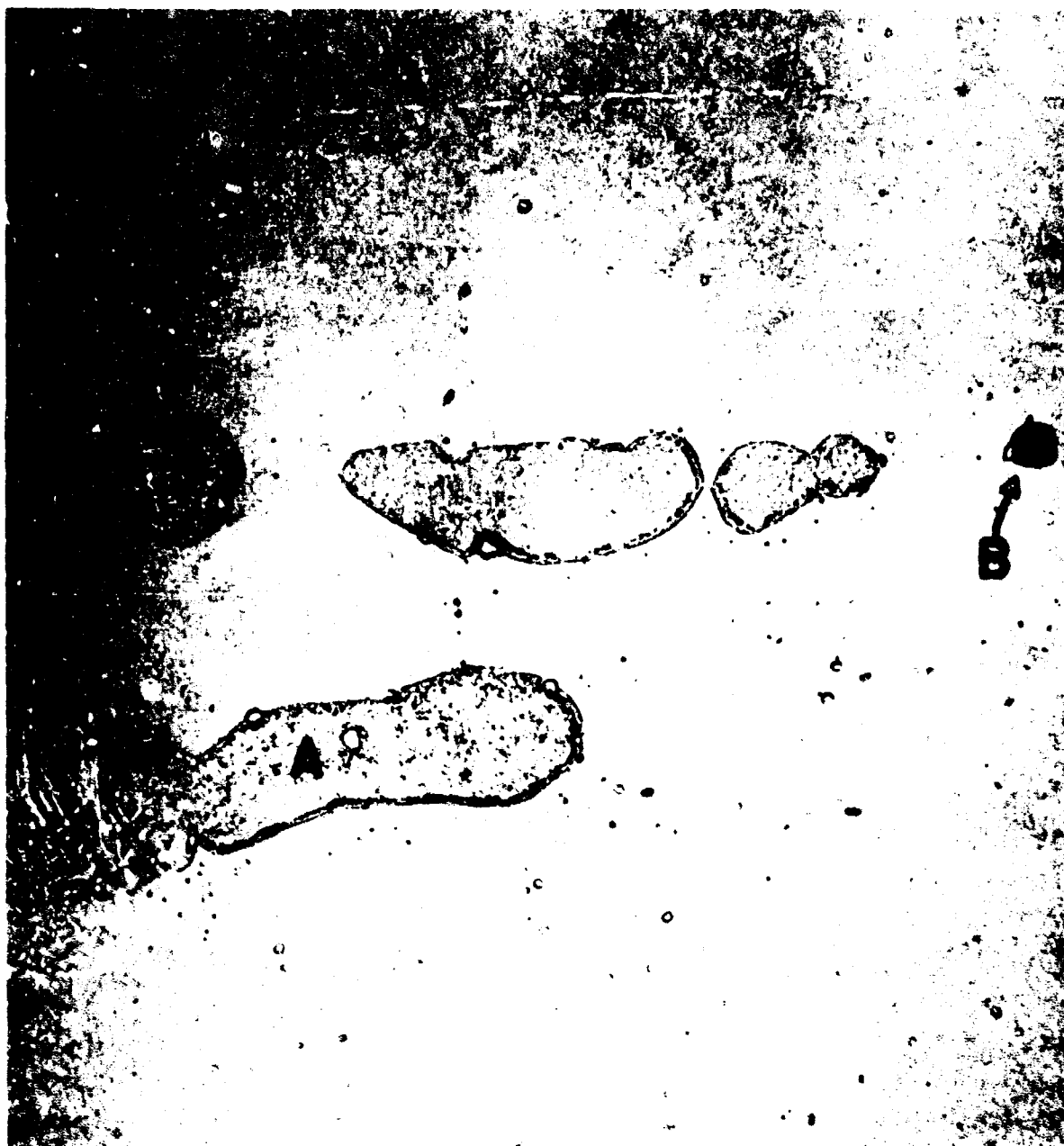
SECTIONS OF 1/8" DIAMETER SHORT TRANSVERSE TENSILE
SPECIMENS OF 7075-T6 STRESSED TO 75% Y.S. AND HELD
AT VARIOUS POTENTIALS IN ACIDIFIED NaCl/ALCl₃ SOLUTION.

Figure 18

Figure 19

Shows the structure of the uncorroded 7075-T6. The grey structures at "A" represent particles that oxidized during the formation of the replica. The dark structure at "B" represents a particle extracted intact. The difference in behavior suggests that "A" and "B" were not the same type of particle.

In preparing the micrographs in Figures 19 to 24, specimens were metallographically polished and then corroded, with and without cathodic protection. After corrosion, the specimens were cleaned in hot chromic-phosphoric acid stripping solution, 20 g CrO_3 and 35 ml H_3PO_4 (sp. gr. 1.69) per liter, for 30 minutes at 90°C to remove corrosion product. The replicas were formed in a 3% tartaric acid solution adjusted to pH 5 with ammonium hydroxide. This type of replica has the unique characteristic of penetrating pits and crevices and of including particles on the surface.



S. No. 320831

Oxide Replica

10,000X

Figure 19

Figure 20

7075-T6 allowed to corrode freely for 24 hours. The surface was highly attacked with many deep pits that penetrated and undermined the surface. "A" is the bottom of a pit, and the dark area "B" is a region where the electron beam passed through several (usually three) layers of the replica formed by the front surface, the side wall and the bottom of a pit. The general pattern of attack was cubic as indicated by "C". Occasional particles, "D", remained unattacked; to some degree these particles appeared to be associated with pits, possibly acting as cathodes. The grey particles shown at "A" in Figure 15 appear to have dissolved out.



S. No. 320931-E2

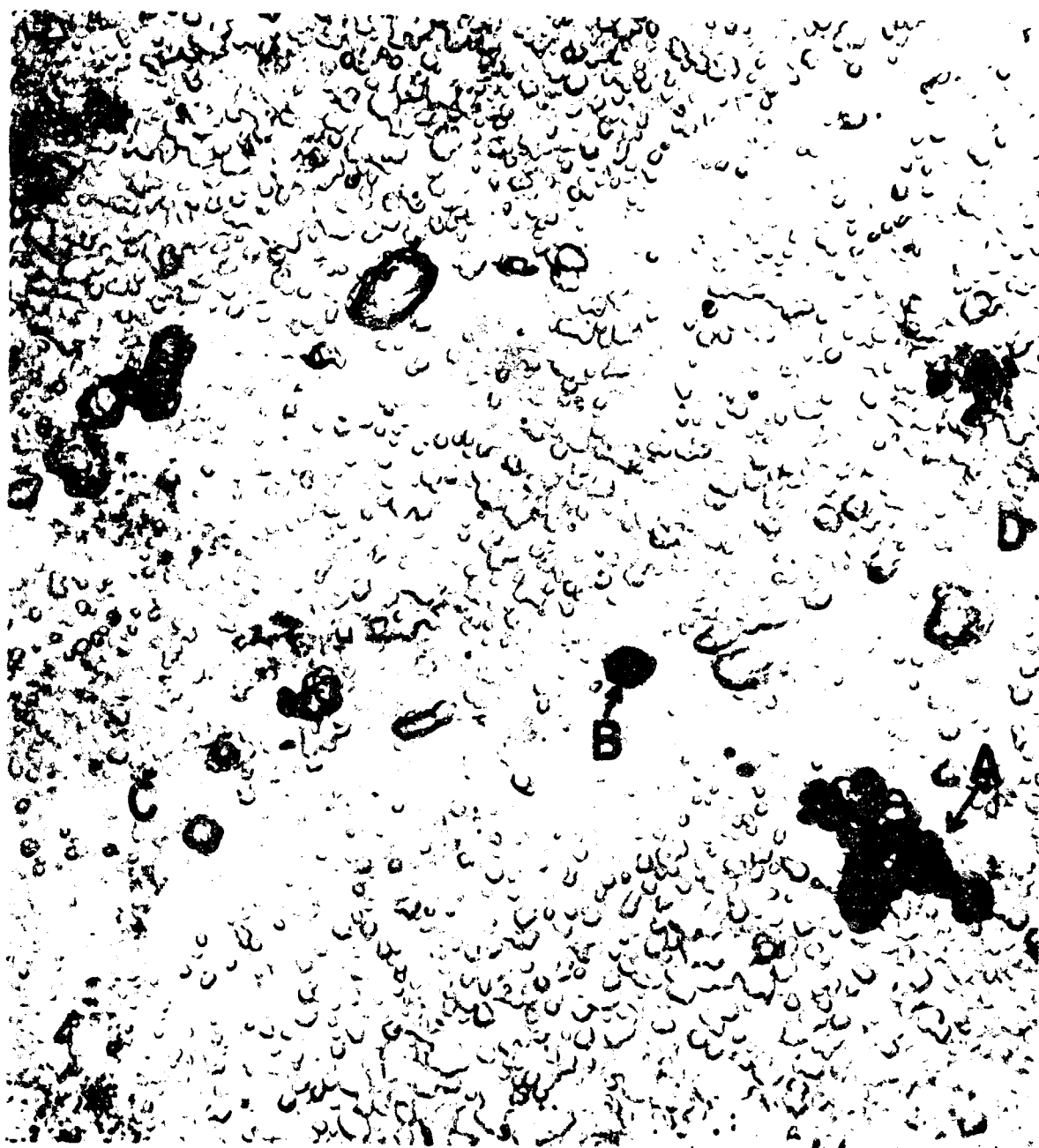
Oxide Replica

10,000X

Figure 20

Figure 21

7075-T6 exposed for 24 hours at a potential of -1.15 v. Shows considerable attack, with numerous large pits and occasional small pits "A". The general attack is no longer discretely cubic. Many particles have been dissolved but occasional particles "B" remain intact. The grain boundary extending from "C" to "D" also shows evidence of attack, largely at particles.



S. No. 320831-E3

Oxide Replica

10,000X

Figure 21

Figure 22

7075-T6 exposed for 24 hours at a potential of -1.25 v. Shows relatively mild attack with occasional large pits "A". Again indications of undermining are seen at "B".



S. No. 320831-E5

Oxide Replica

10,000X

Figure 22

Figure 23

7075-T6 exposed for 24 hours at a potential of -1.25 v; different field but same specimen shown in Figure 18. Shows relatively mild attack. The particle "A" has been attacked leaving some corrosion products. "A" appears to have been the same type of particle as was indicated by "A" in Figure 15.



S. No. 320831-E5

Oxide Replica

10,000X

Figure 23

Figure 24

7075-T6 exposed for 24 hours at a potential of -1.32 v. The amount of attack in the background is very mild and comparable to that shown in Figures 18 and 19, but is definitely more than the unexposed specimen shown in Figure 15. The absence of large or small pits is the outstanding feature because pitting occurred at all potentials less negative than -1.32 v. The particles "A" have been attacked similar to those shown in Figure 19. The particle at "B" was unattacked. The grain boundary attack at "C" is very mild compared to that shown in Figure 17.



S. No. 320831-E6

Oxide Replica

10,000X

Figure 24

Figure 25

Diagrams showing the solution potential of selected alloys in the aluminum solid solution region of the Al-Mg-Zn-Cu system. The potentials were measured in the acidified (pH 1.0) sodium + aluminum chloride solution used for the cathodic protection studies, and are referred to the saturated calomel reference electrode. These specimens were solution heat treated and cold water quenched.

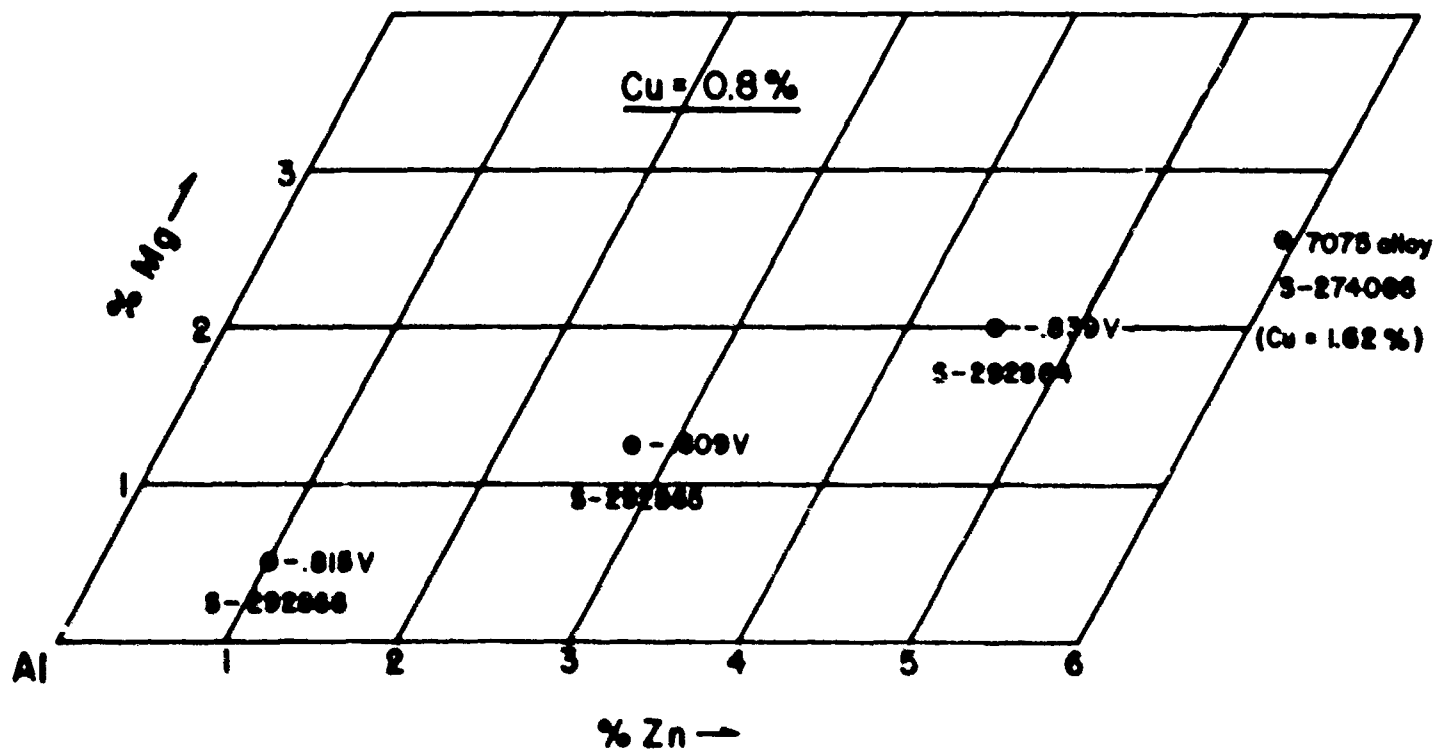
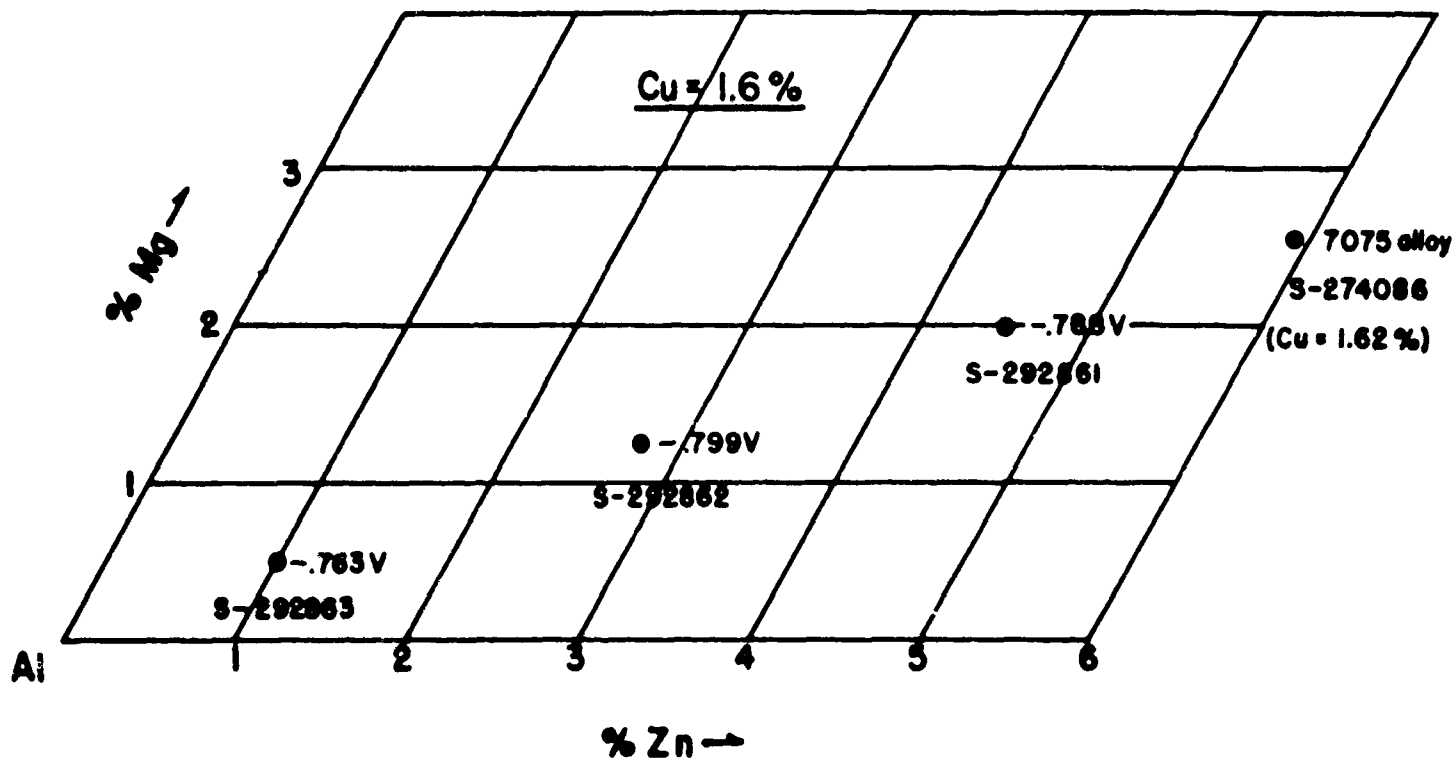


Figure 25

Figure 26

Diagram showing the solution potential of selected alloys in the M-phase region of the Al-Mg-Zn-Cu system. The potentials were measured in the acidified (pH 1.0) sodium + aluminum chloride solution used for the cathodic protection studies, and are referred to the saturated calomel reference electrode. (Perspective diagram after Strawbridge, Hume - Rothery, and Little).

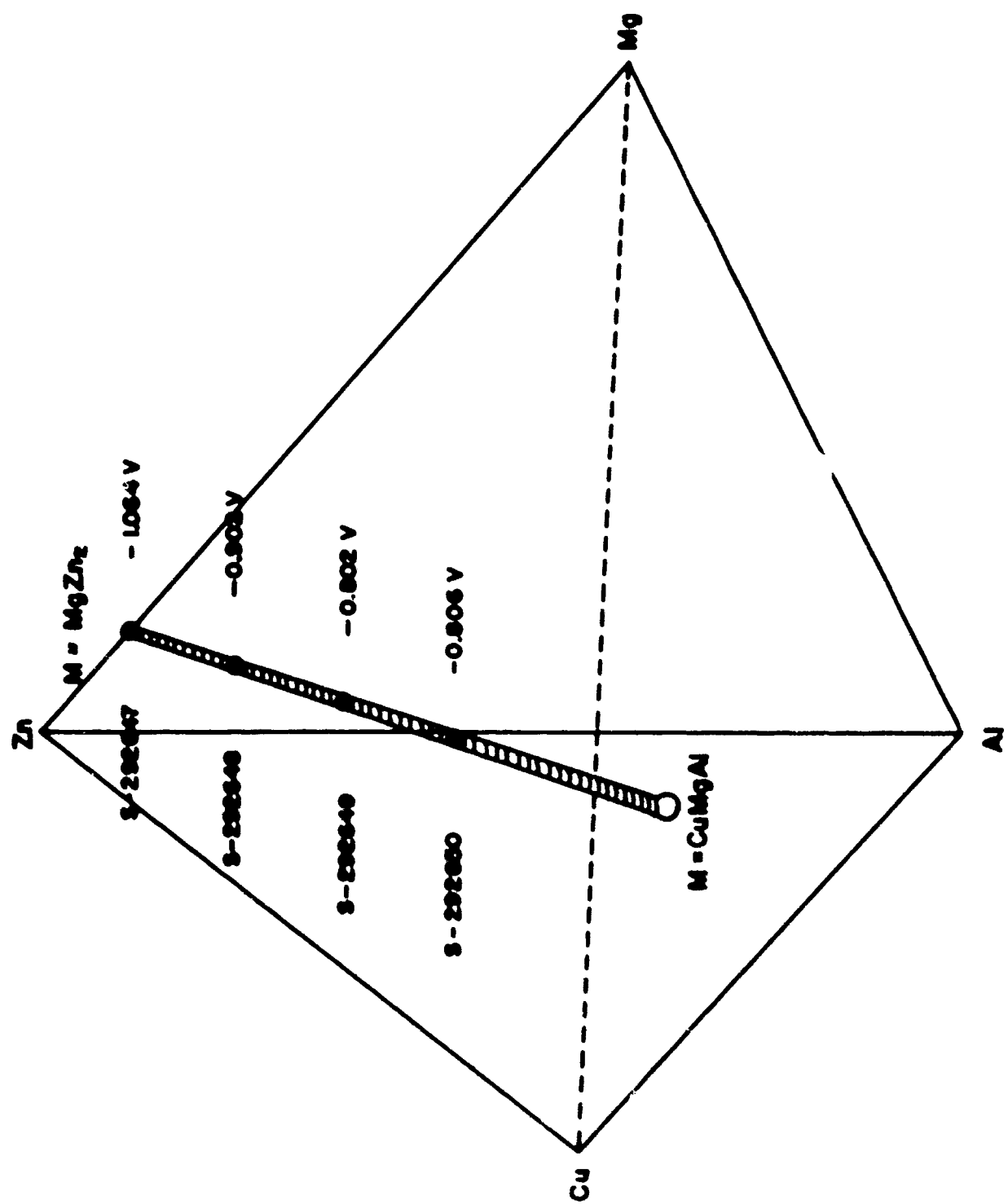


Figure 28

Figure 27

Cathodic protection of an M-phase alloy (100% MgZn_2) in acidified (pH 1.0) sodium + aluminum chloride solution, as evaluated by weight loss measurements.

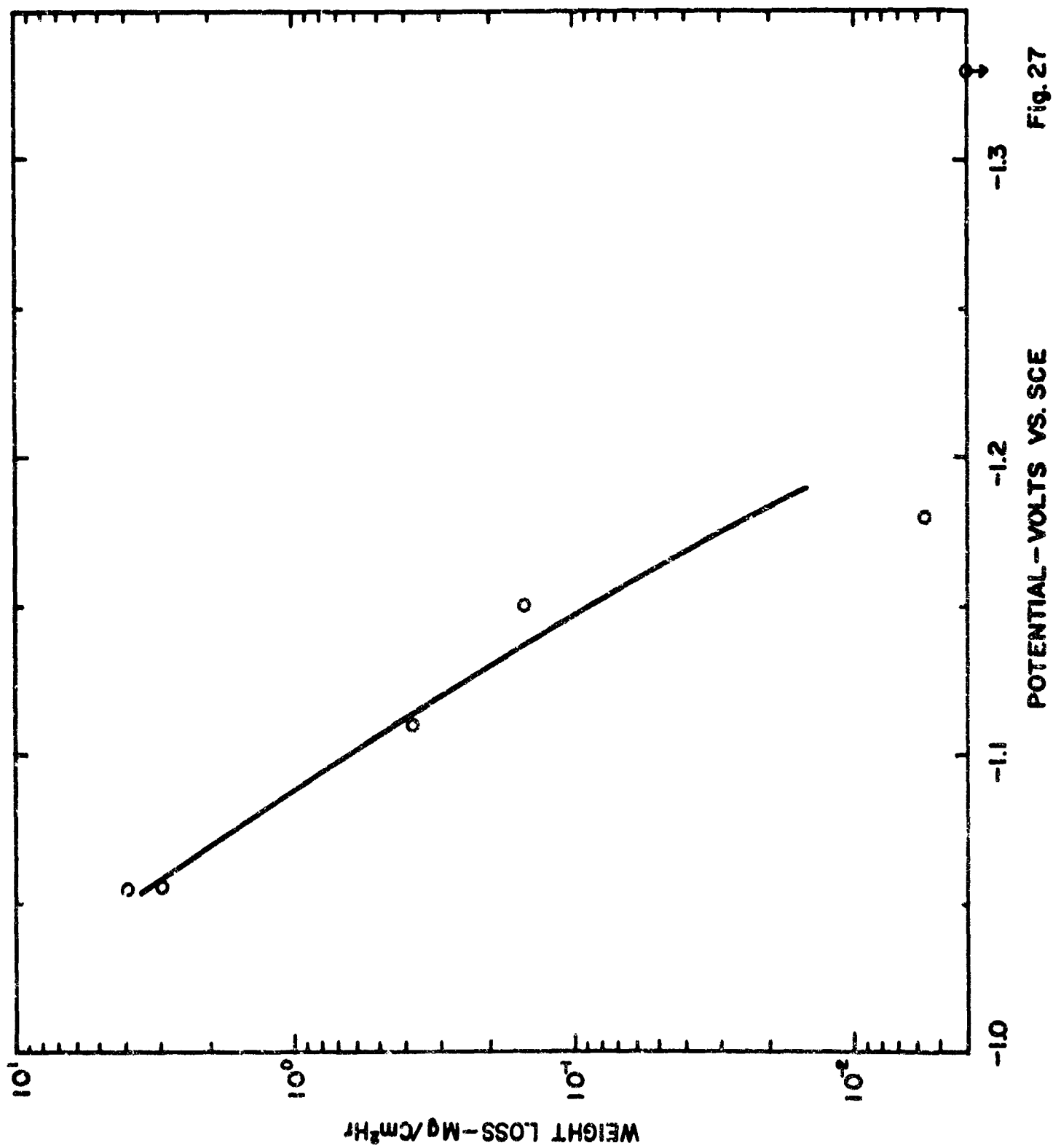


Fig. 27

Figure 28

Effect of pH on time to failure for 7075-T6 specimens stressed to 75% of the yield strength and allowed to freely corrode in chloride solutions. Closed circle denotes 1.6 N NaCl; open circle denotes 1 N NaCl with AlCl_3 at 0.2 mole per liter or at the solubility limit set by precipitation of $\text{Al}(\text{OH})_3$.

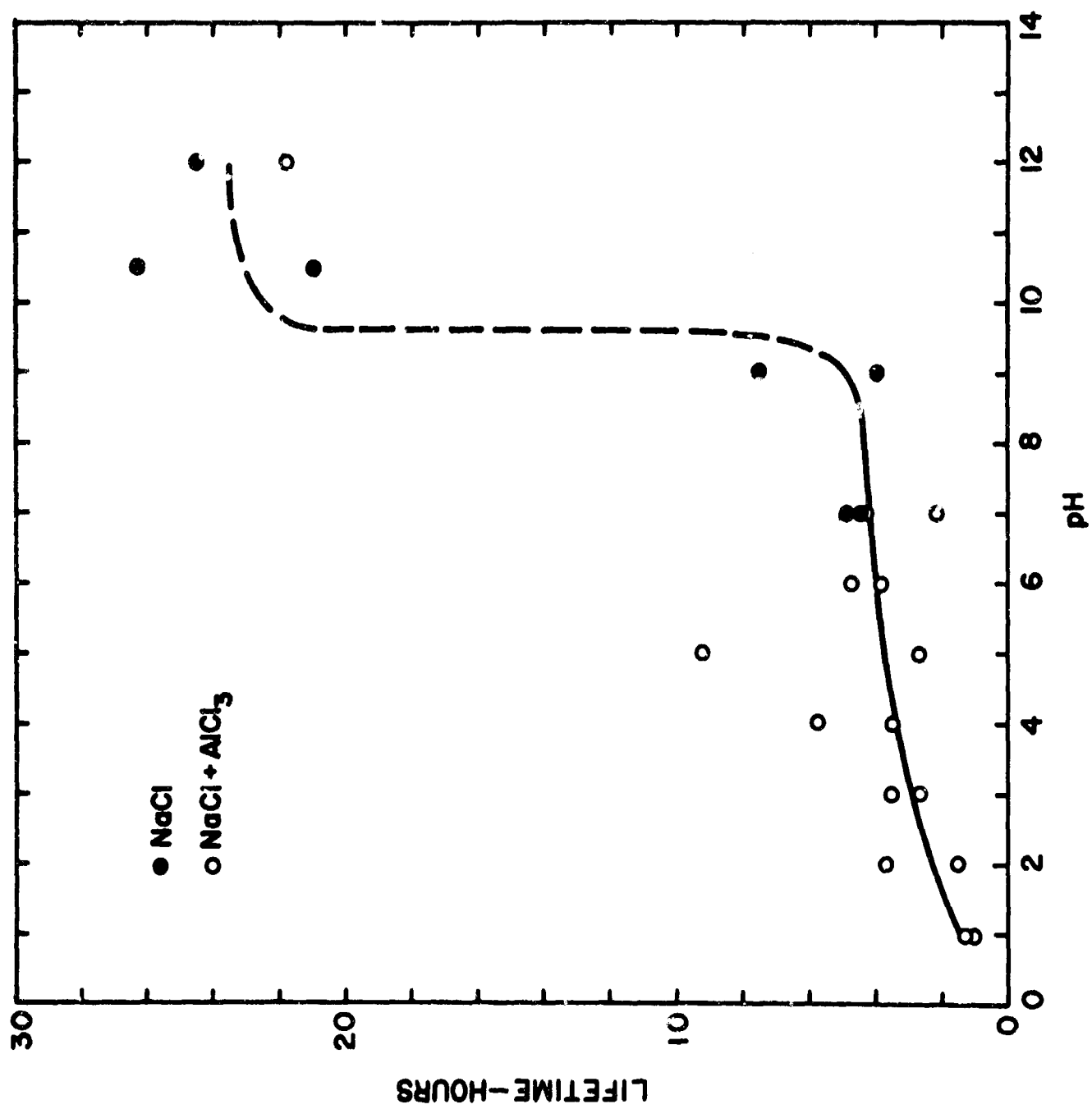
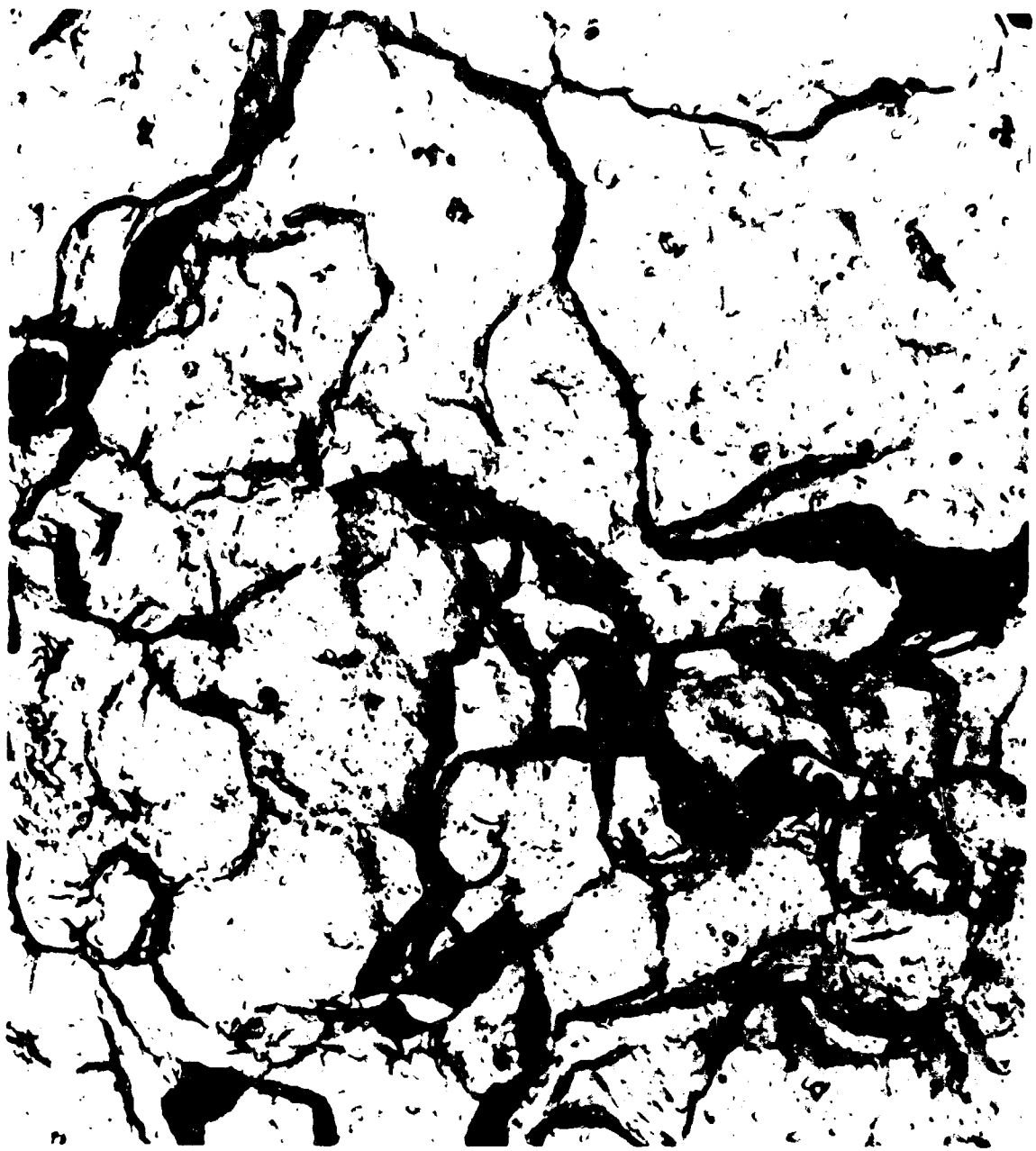


Fig. 28

Figure 29

Electron micrograph showing intergranular corrosion in the bright portion of the fracture of a 7075-T6 specimen exposed to 1.6 N NaCl at pH 7.



320413-N39

Oxide Replica

5,000X

Figure 29

Figure 30

Electron micrograph showing intergranular corrosion in the bright portion of the fracture for 7075-T6 specimen exposed to 1.6 N NaCl at pH 12.



320713-N15

Oxide Replica

5,000X

Figure 30

Figure 31

Graph showing the effect of pH on the rate of cathodic corrosion of 7075-T6. Closed circles denote 1.6 N NaCl at pH 7; open circles denote solution containing 1.0 N NaCl + 0.2 moles per liter AlCl_3 at pH 1.

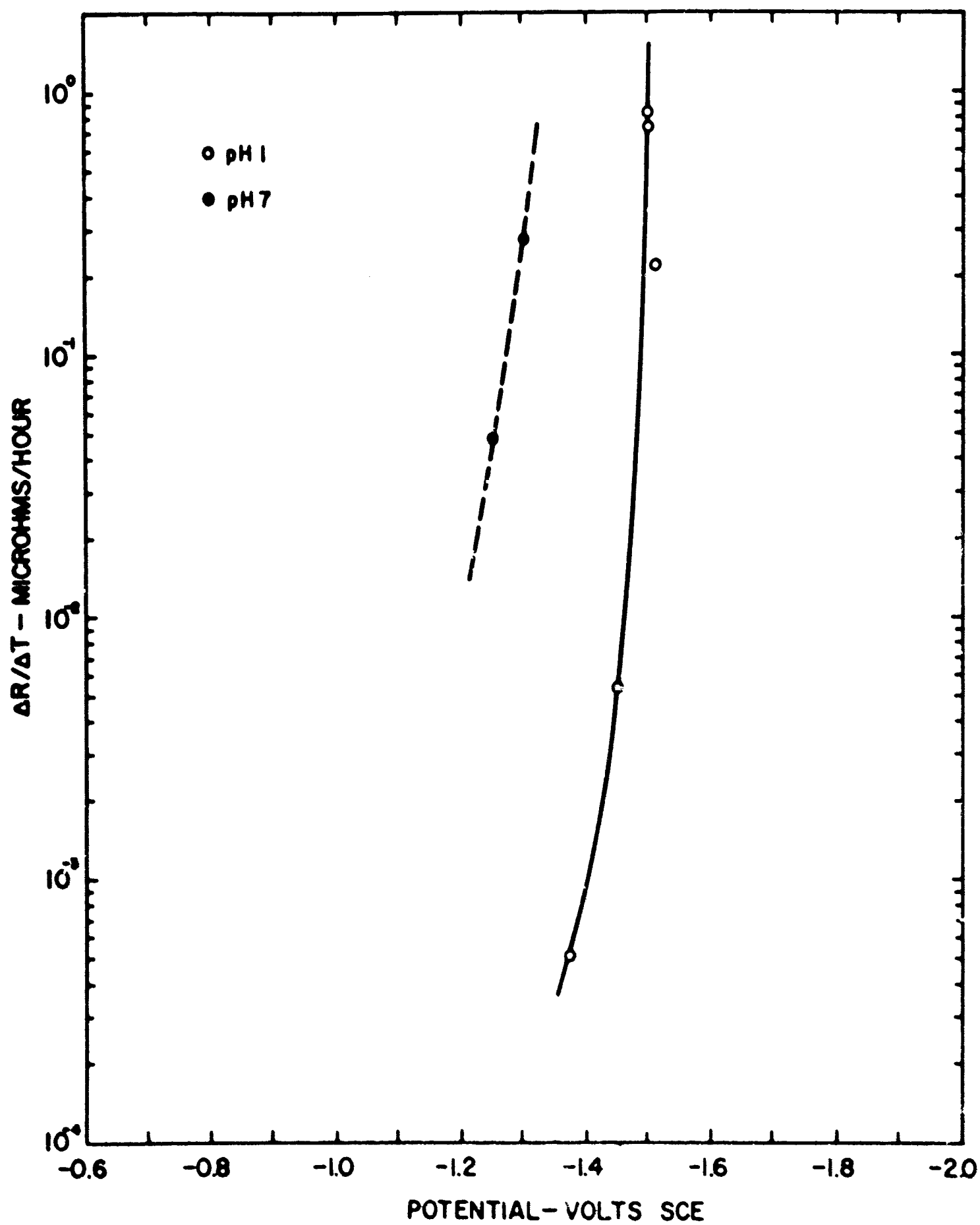


Fig. 31

Figure 32

Effect of dissolved corrosion product on the
current associated with cathodically protected specimens.

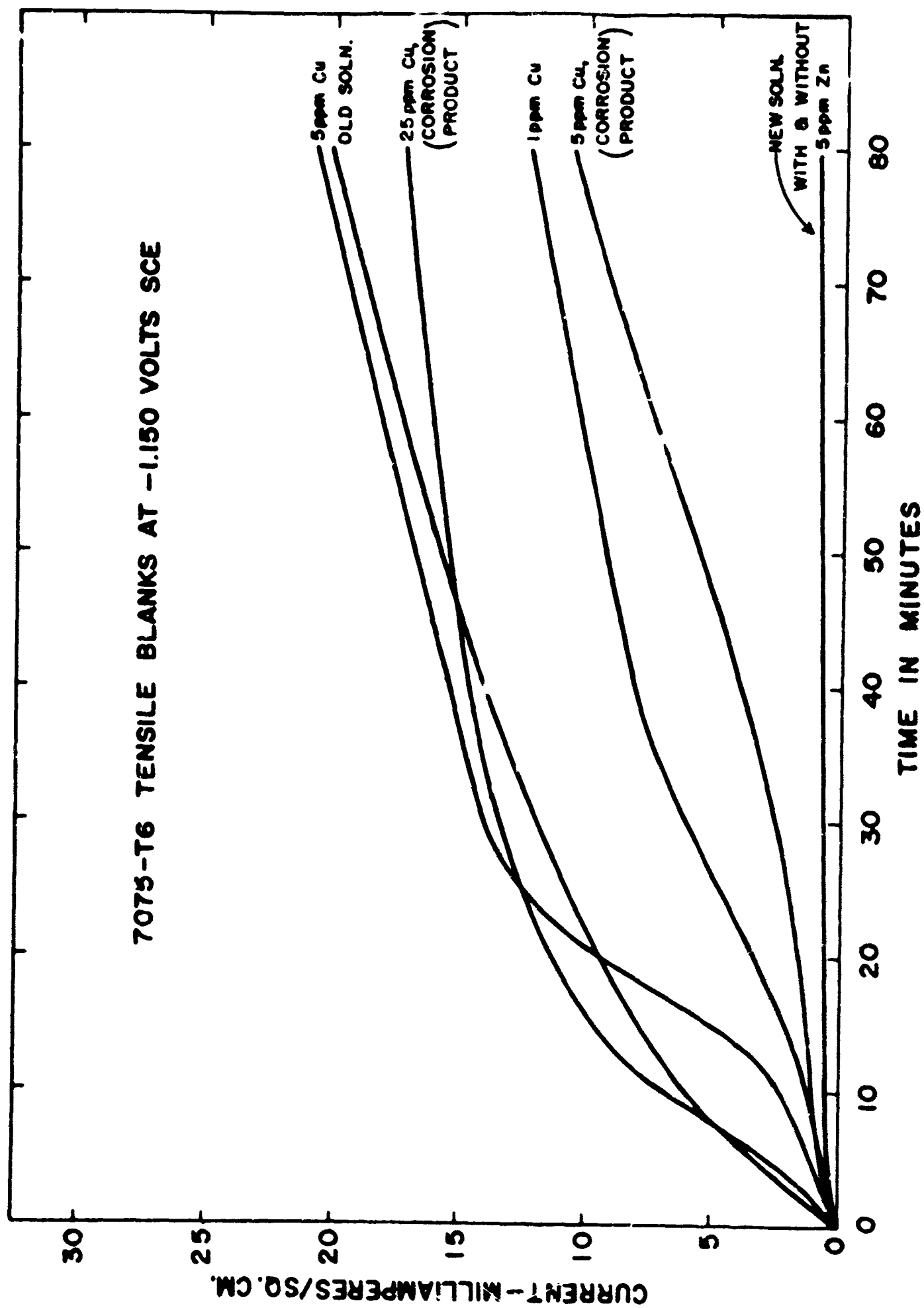


Fig. 32

APPENDIX I

Where corrosion is uniform the relation between resistance change and corrosion rate of a cylindrical specimen can be derived rather easily, starting with the relation between resistance and the resistivity ρ

$$R = \frac{\rho L}{A} = \frac{\rho L}{\pi r_o^2} \quad (1)$$

where R is the resistance, L is the length and r_o is the original radius of the specimen. If the radius is reduced to r by uniform corrosion after an exposure period of t, then the change in resistance is

$$\Delta R = \frac{\rho L}{\pi r^2} - \frac{\rho L}{\pi r_o^2} \quad (2)$$

Differentiating equation (2) with respect to time

$$\frac{d\Delta R}{dt} = - \frac{2\rho L}{\pi} \frac{1}{r^3} \frac{dr}{dt} \quad (3)$$

$$- \frac{dr}{dt} = \frac{\pi r^3}{2\rho L} \frac{d\Delta R}{dt} \quad (4)$$

from equation (2)

$$r = \left[\frac{\rho L r_o^2}{\pi r_o^2 \Delta R + \rho L} \right]^{1/2} \quad (5)$$

substituting equation (5) into (4) gives

$$- \frac{dr}{dt} = \frac{\pi}{2\rho L} \left[\frac{1}{\frac{1}{r_o^2} + \frac{\pi}{\rho L} \Delta R} \right]^{3/2} \frac{d\Delta R}{dt} \quad (6)$$

Where corrosion is not uniform, it is necessary to take account of the non-uniformity by use of some type of correction factor.

APPENDIX II

In the initial phase of the investigation, anodic polarization was considered as a technique for selecting electrolytes to provide a wide range of stress corrosion performance for the various aluminum alloys and tempers, which were under consideration. This technique was not pursued after it became apparent that the major part of the contract work would be devoted to the cathodic protection of 7075-T6 and -T73 in the acidified chloride solution.

One feature of the anodic polarization curves, which deserves mention, is shown in Figure 33. It is evident that the breaks in the anodic polarization curve correlate well with the stress corrosion resistance expected for three different tempers of 7075. As indicated in the facing sheet for Figure 33, an anodic pretreatment was employed to develop active sites of attack, and immediately following the pretreatment, the anodic polarization curve was recorded, using a rapid scanning rate to minimize the effects of film repair.

Figure 33

Anodic polarization of cold water quenched 7075. The curves show two branches each of which is nearly linear. The current corresponding to the break or intersection of the two branches of the polarization curve correlates with the expected resistance to stress corrosion. The -T73 temper shows the lowest current at the break and has outstanding resistance to stress corrosion. The following procedure was used:

Electrolyte	3-1/2% NaCl
Pretreatment	20 minutes at 10 milliamperes per square centimeter.
Scanning Rate	200 millivolts per minute positive direction

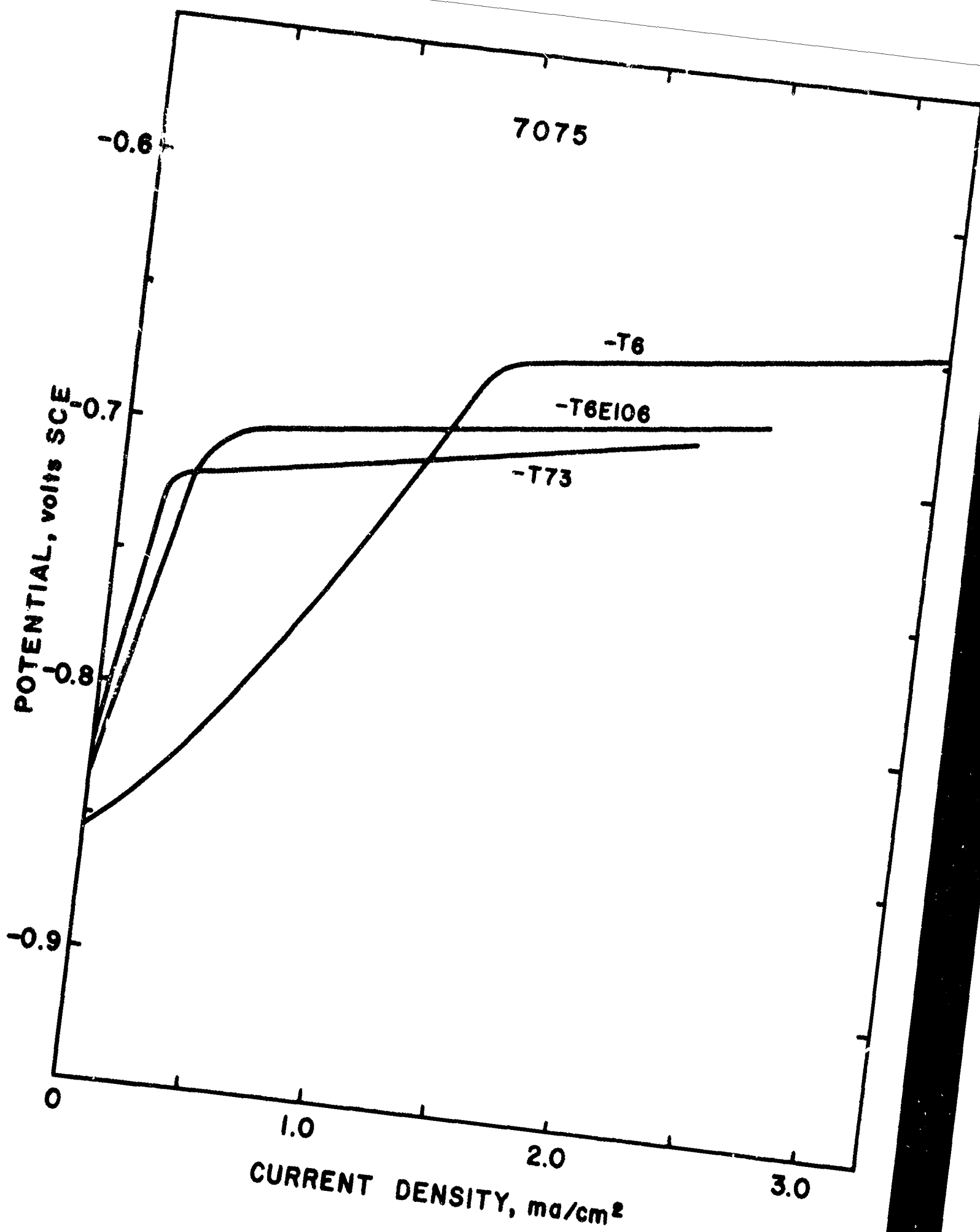


Figure 33

ERRATA - Investigation of the Mechanism of Stress
Corrosion of Aluminum Alloys. Bureau of Naval Weapons
Contract NOW 64-0170-c. Final Report,
December 6, 1963, to February 6, 1965.

1. Page 3, paragraph 3, line 3 - insert "as" between "added" and "50."
2. Page 23, paragraph 1, line 4 - change "Kologyrkin" to "Kolotyrkin."
3. Page 23, paragraph 2, line 7 - change "importnat" to "important."
4. Table III, next to last entry - change "-1290" to "(-1290*)."
5. Figure 9, facing sheet caption - add "The stressed specimen was stressed to 75% of the yield strength."
6. Figure 20, facing sheet caption, last sentence - change to "Any gray particles like those shown at "A" in Figure 19 appear to have dissolved out."
7. Figure 23, facing sheet caption, line 3 - change Figure 18 to Figure 22.
8. Figure 23, facing sheet caption, line 6 - change Figure 15 to Figure 19.
9. Figure 24, facing sheet caption, line 3 - change Figures 18 and 19 to Figures 22 and 23.
10. Figure 24, facing sheet caption, line 5 - change Figure 15 to Figure 19.
11. Figure 24, facing sheet caption, lines 7 and 8 - change "The particles at "A" have been attacked. Originally these particles were similar to those shown at "A" in Figure 19."
12. Figure 24, facing sheet caption, line 11 - change Figure 17 to Figure 21.
13. Figure 28 - The data point at pH 12 shown as an open circle should be a solid circle.

ARCHIVE COPY